SAND2020-8734R

A GENERAL FRAMEWORK FOR SUBSTRUCTURING-BASED DOMAIN DECOMPOSITION METHODS FOR MODELS HAVING NONLOCAL INTERACTIONS

GIACOMO CAPODAGLIO*, MARTA D'ELIA†, MAX GUNZBURGER‡, PAVEL BOCHEV§, MANUEL KLAR¶, AND CHRISTIAN VOLLMAN‖

Abstract. A rigorous mathematical framework is provided for a substructuring-based domain-decomposition approach for nonlocal problems that feature interactions between points separated by a finite distance. Here, by *substructuring* it is meant that a traditional geometric configuration for local partial differential equation problems is used in which a computational domain is subdivided into non-overlapping subdomains. In the nonlocal setting, this approach is *substructuring-based* in the sense that those subdomains interact with neighboring domains over interface regions having finite volume, in contrast to the local PDE setting in which interfaces are lower dimensional manifolds separating abutting subdomains. Key results include the equivalence between the global, single-domain nonlocal problem and its multi-domain reformulation, both at the continuous and discrete levels. These results provide the rigorous foundation necessary for the development of efficient solution strategies for nonlocal domain-decomposition methods.

Key words. Nonlocal models, domain decomposition, finite element methods

AMS subject classifications. 34B10, 65M60, 45P05, 45A99, 65R99

1. Introduction.

Nonlocal models have become a popular alternative to partial differential equation (PDE) models due to their ability to describe effects that PDEs fail to capture. In particular, a nonlocal model can describe multiscale and anomalous behavior for applications that exhibit hierarchical features that cannot be reproduced by a classical model. These applications include, among others, subsurface transport [9, 49, 50], image processing [10, 17, 30, 36], multiscale and multiphysics systems [3, 7], magnetohydrodynamic [48], finance [47, 46], and stochastic processes [11, 19, 38, 40, 41].

The general class of nonlocal models we consider are characterized by integral operators having the form

$$\mathcal{L}u(\boldsymbol{x}) = \int_{B_\delta(\boldsymbol{x})} (u(\boldsymbol{y}) - u(\boldsymbol{x}))\gamma(\boldsymbol{x},\boldsymbol{y})\, d\boldsymbol{y}, \tag{1}$$

where $B_\delta(\boldsymbol{x})$ denotes the ball (usually Euclidean) centered at $\boldsymbol{x}$ with radius δ (usually referred to as the *horizon* or *interaction radius*) and $\gamma(\boldsymbol{x},\boldsymbol{y})$ is an application-dependent kernel function (usually symmetric in its arguments and nonnegative) that determines the regularity properties of the solution. The nonlocality inherent in (1) is clear: points $\boldsymbol{x}$ interact with all points $\boldsymbol{y}$ located within a distance δ. Compared

*Department of Scientific Computing, Florida State University, Tallahassee FL 32306. Present address: Computational Physics and Methods, Los Alamos National Laboratory, Los Alamos NM 87545; gcapodaglio@lanl.gov.

†Computational Science and Analysis, Sandia National Laboratories, Livermore CA 94550; mdelia@sandia.gov

‡Department of Scientific Computing, Florida State University, Tallahassee FL 32306; mgunzburger@fsu.edu.

§Center for Computing Research, Sandia National Laboratories, Albuquerque NM 87321; pbboche@sandia.gov

¶Department of Mathematics, Universität Trier, 54296 Trier, Germany; klar@uni-trier.de

‖Department of Mathematics, Universität Trier, 54296 Trier, Germany; vollmann@uni-trier.de

to that for the local PDE setting, the integral form clearly reduces regularity requirements on the solution and allows for the capture of long-range interactions.

However, the utilization of nonlocal models in applications that result in improved predictive capabilities is hindered by several modeling and numerical challenges. Relevant to this work there are, e.g., the unresolved treatment of nonlocal interfaces [2, 13], the nontrivial prescription of nonlocal volume constraints (the nonlocal counterpart of boundary conditions) [16, 24], and the fact that computational costs attendant to the use of nonlocal problems may become prohibitive as the extent of the nonlocal interactions increases; see, e.g., [18, 23] for variational methods and [14, Chapter 7] for mesh-free methods. Other critical challenges are related to the uncertain nature of model parameters; in fact, modeling parameters such as δ and those characterizing the kernel, applied forces, and/or sources can be non-measurable, sparse, and/or subject to noise. Research on such topics is very active (see, e.g., [6, 5, 20, 21, 22, 17, 31, 42, 43, 44, 52]) but further consideration of them is beyond the scope of this work.

Here, we focus on the treatment of nonlocal interfaces and, notably on the design of nonlocal domain-decomposition (DD) formulations with the aim of reducing computational costs by increasing the parallel concurrency in the numerical solution of nonlocal problems. Specifically, the goal is to address the high computational cost associated with nonlocal models by providing a foundational algorithmic framework for their parallel solution, mirroring that of successful parallel algorithms for DD for PDEs such as, e.g., Finite Element Tearing and Interconnecting (FETI) [29] and other approaches [37, 51].

This work is part of a comprehensive effort by the authors to fill the theoretical and practical gaps in the current understanding of nonlocal interfaces (both physical ones and those created by DD solution algorithms) by developing a rigorous nonlocal interface theory for nonlocal diffusion (see the preliminary work [13]), including pure fractional diffusion, and nonlocal mechanics. Our ultimate goal is to design efficient and scalable DD solvers to unlock the full potential of nonlocal models. To this end, as is often done in nonlocal modeling, we take inspiration from the vast literature about classical DD methods for PDEs. Unfortunately, the extension of local DD methods to nonlocal models is a nontrivial task: nonlocality introduces many challenges and limitations. Some of these challenges are shared with local DD methods. An example of a shared challenge is the proper treatment of *floating subdomains*[1] which require special attention due to the singularity of the discretized equations on such subdomains.

However, other challenges are unique to the nonlocal setting and require new approaches that have no analogs in the local setting. For example, in the local PDE setting, a typical class of DD methods commonly starts by breaking the computational domain into non-overlapping subdomains, a process we refer to as *substructuring of the domain*. These subdomains interact only through their shared boundaries on which one usually imposes some appropriate continuity conditions. Although one starts from the same initial geometric configuration in which the domain is substructured into non-overlapping subdomains, inherent nonlocal interactions between the subdomains force one to expand these subdomains to include parts of neighboring subdomains having nonzero volume, causing an overlap of a thickness determined by the interaction radius

[1] In a multi-domain setting, floating domains are subdomains of the decomposition that are either internal (they do not share boundaries with the physical boundary) or share boundaries only with parts of the physical boundary at which Neumann-type conditions are prescribed. In this context "floating" refers to the fact that these domains either do not have volume constraints because they are internal, or have partial constraints of Neumann type.

δ. This overlap is required because, in the nonlocal setting, it is not possible to define subdomain problems simply by restricting the global operator to the subdomains. For this reason we refer to our approach as being *substructuring-based*. It is important to point out that the thickness of the overlap regions depends solely on the *modeling* parameter δ and is unrelated to the discretization method employed and, in particular, to the grid size. As a result, discretization of the decomposed nonlocal problem requires special care because the overlapping regions induced by the decomposition do not, in general, match the underlying mesh.

The current state of the art of nonlocal DD methods is very limited, with [1] being perhaps the most relevant work. In that paper, the authors consider a simple two-domain configuration and develop a variational approach to DD based on adding an interface equation and a new variable that lives on the overlap between the subdomains, while using test functions that vanish on the interface for each subdomain. Decoupling is achieved by solving a Schur-complement problem for the interface variable, similar to a conventional FETI scheme. The subproblem definition in [1] does not consider multi-domain configurations nor does it consider floating subdomains. As a result, it is not clear how one extends that approach to the general multi-domain case.

In this paper we formulate a general framework for nonlocal DD problems with the central goal being that

(2) *the discrete solution obtained via the DD approach is identical to the discrete solution obtained for the parent single domain.*

As already mentioned, we refer to our approach as "substructuring-based" because, much like as it is in standard non-overlapping DD, the subdomains interact only through their shared interfaces. Of course, the key difference is that in the nonlocal setting these shared interfaces are nonlocal, i.e., they are regions having finite volumes as opposed to the local case in which interfaces are lower-dimensional manifolds.

The main contributions of this paper are as follows.

- We introduce a systematic way to decompose the domain given an existing mesh for the single-domain problem and we discuss ways to make the decomposed domains compatible with the given mesh. Specifically, we provide a recipe for decomposing the domain that prevents integration over partial (cut) finite elements by using approximate neighborhoods in a manner such that the equivalence of the decomposed solution and the single-problem one is not compromised.
- We formulate a continuous nonlocal DD system of subdomain problems and prove that it is equivalent to the single-domain problem. The key ingredient is the appropriate definition of indicator functions that keep track of the number of overlapping subdomains.
- We define a Galerkin finite element discretization of the nonlocal DD problem and prove that it is equivalent to the discretization of the single-domain domain problem effected using the same type of finite element functions. This equivalence holds for the finite-dimensional variational formulation and for the corresponding matrix form.

Our nonlocal DD formulation provides a mathematical foundation for the development of a range of efficient numerical algorithms for the parallel solution of nonlocal problems that mirror existing approaches for local problems. For example, treating the nonlocal interface equations as constraints and using Lagrange multipliers to enforce them lends itself to the development of nonlocal FETI [29] or Arlequin [25] like

algorithms. Alternatively, one can choose to view these coupling conditions as an an optimization objective and treat the subdomain equations as constraints. Such an approach would lead to nonlocal optimization-based DD methods that are nonlocal counterparts of the methods in [32, 33, 34].

It should be noted though that realizing the potential of our DD framework to reduce the computational burden of solving nonlocal problems requires the ratio between δ and the linear size of the subdomains to be smaller than 1, i.e., we target problems for which the extent of the nonlocal interactions is much smaller than the diameter of the domain. Such problems arise in several engineering applications such as, e.g., nonlocal mechanics, and are the main motivator for this work. In contrast, for applications described by nonlocal operators with infinite interactions, a DD approach may not be as effective because the interaction regions would span a portion of the domain that is of the same size (or even larger) than the domain itself.

Finally, we mention that often one may be given a decomposition of Ω into a *few* subdomains which is constructed to follow well-defined geometric entities, e.g., a wing and a fuselage, or different media properties, e.g., different diffusion coefficients, within Ω. Such "physically"-motivated DDs typically arise in the context of *mesh tying* [35, 45] in which a complex geometric entity is broken into smaller parts to enable efficient mesh generation. In contrast, here we focus on DD as a means for faster and more efficient parallel solution methods for nonlocal problems in which case the number of the subdomains is very large and they do not generally follow any "physics"-motivated interfaces.

Outline of the paper. The paper is organized as follows. In Section 2, we recall the variational formulation of a single-domain volume-constrained nonlocal Poisson problem and briefly describe its discretization via finite element methods. In Section 3, we introduce the continuous formulation of a multi-domain nonlocal DD method and prove its equivalence to the single-domain problem presented in Section 2. Section 4 explains how we address the decomposition problem by formulating rules for the construction of the subdomains and their interaction regions that guarantee the equivalence of the DD and the single-domain problems. In the same section we also introduce the discretized subproblems and their matrix forms and show their equivalence to the underlying single-domain formulation. Concluding remarks are provided in Section 5. In Appendix A we report the proof of the main result of this work. In Appendix B, we further elucidate the equivalence between the multi-domain formulation and the single-domain problem and illustrate the application of the nonlocal DD framework. Specifically, we use the framework developed in this work along with a FETI solution approach to obtain, for a very simplified setting, illustrative numerical examples of nonlocal DD problems.

2. A nonlocal (single-domain) volume-constrained problem and its finite element discretization. For simplicity, in this work, we consider the two-dimensional case. Let $\widehat{\Omega}$ denote a bounded, open subset of $\Re^2$. For any $\delta > 0$, often referred to as the *horizon* or *interaction radius*, we define the associated *interaction domain* as the closed region

$$\Gamma_{interaction} = \{\boldsymbol{y} \in \Re^2 \setminus \widehat{\Omega} \,:\, |\boldsymbol{x} - \boldsymbol{y}| \leq \delta \text{ for some } \boldsymbol{x} \in \widehat{\Omega}\}\,. \tag{3}$$

The interaction domain is split into two disjoint parts Γ and $\Gamma_{Neumann}$, where Γ is a nonempty closed domain, whereas $\Gamma_{Neumann}$ is allowed to be empty. Thus, we have that $\Gamma \cup \Gamma_{Neumann} = \Gamma_{interaction}$ and $\Gamma \cap \Gamma_{Neumann} = \emptyset$, where $\Gamma_{Neumann}$ is open along its common boundary with Γ. Also, note that $\Gamma_{interaction}$ and therefore also Γ

and $\Gamma_{Neumann}$ depend on δ, even though that dependence is not explicitly indicated. Figure 1-left illustrates this geometric configuration.[2]

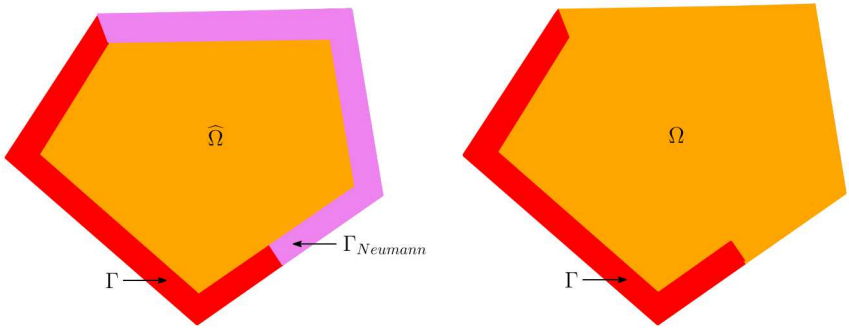

FIG. 1. *Left: A domain $\widehat{\Omega}$ and its associated interaction domain $\Gamma \cup \Gamma_{Neumann}$ on which Dirichlet and Neumann volume constraints are imposed on Γ and $\Gamma_{Neumann}$, respectively. Right: the domain $\Omega = \widehat{\Omega} \cup \Gamma_{Neumann}$.*

The strong formulation of a nonlocal volume-constrained Poisson problem is given by [18, 26, 27, 28][3]

$$
\begin{cases}
-2\displaystyle\int_{\widehat{\Omega}\cup\Gamma\cup\Gamma_{Neumann}} \big(u(\boldsymbol{y}) - u(\boldsymbol{x})\big)\gamma(\boldsymbol{x},\boldsymbol{y})d\boldsymbol{y} = f_{\widehat{\Omega}}(\boldsymbol{x}) & \boldsymbol{x} \in \widehat{\Omega} \quad (a)\\
u(\boldsymbol{x}) = g(\boldsymbol{x}) & \boldsymbol{x} \in \Gamma \quad (b)\\
2\displaystyle\int_{\widehat{\Omega}\cup\Gamma\cup\Gamma_{Neumann}} \big(u(\boldsymbol{y}) - u(\boldsymbol{x})\big)\gamma(\boldsymbol{x},\boldsymbol{y})d\boldsymbol{y} = f_{Neumann}(\boldsymbol{x}) & \boldsymbol{x} \in \Gamma_{Neumann}, \quad (c)
\end{cases} \tag{4}
$$

where $f_{\widehat{\Omega}}(\boldsymbol{x})$, $f_{Neumann}(\boldsymbol{x})$, and $g(\boldsymbol{x})$ are given functions and $\gamma(\boldsymbol{x},\boldsymbol{y})$ is a given symmetric positive kernel, i.e., $\gamma(\boldsymbol{x},\boldsymbol{y}) = \gamma(\boldsymbol{y},\boldsymbol{x})$ for $\boldsymbol{x}$, $\boldsymbol{y} \in \widehat{\Omega} \cup \Gamma \cup \Gamma_{Neumann}$. Equations (4b) and (4c) are *volume constraints imposed on sets with nonzero measures in* $\Re^2$ which are nonlocal analogues of the Dirichlet and Neumann boundary conditions, respectively, for PDEs. For this reason we refer to (4b) and (4c) as a *Dirichlet volume constraint* and a *Neumann volume constraint*, respectively.

The nonlocal operators in (4a) and (4c) are identical up to a sign so that these equations can be combined to obtain an equivalent, more compact, strong form

$$
\begin{cases}
-2\displaystyle\int_{\Omega\cup\Gamma} \big(u(\boldsymbol{y}) - u(\boldsymbol{x})\big)\gamma(\boldsymbol{x},\boldsymbol{y})d\boldsymbol{y} = f(\boldsymbol{x}) & \boldsymbol{x} \in \Omega\\
u(\boldsymbol{x}) = g(\boldsymbol{x}) & \boldsymbol{x} \in \Gamma,
\end{cases} \tag{5}
$$

where $\Omega = \widehat{\Omega} \cup \Gamma_{Neumann}$, $f(\boldsymbol{x})|_{\widehat{\Omega}} = f_{\widehat{\Omega}}(\boldsymbol{x})$, and $f(\boldsymbol{x})|_{\Gamma_{Neumann}} = -f_{Neumann}(\boldsymbol{x})$. The strong form (5) corresponds to the configuration in Figure 1-right and is used in

[2]Domains such as Γ and $\Gamma_{Neumann}$ in Figure 1-left and therefore also in subsequent figures are stylized versions of their true shapes. For example, because points $\boldsymbol{x}$ interact only with points $\boldsymbol{y} \in B_\delta(\boldsymbol{x})$, where $B_\delta(\boldsymbol{x})$ denotes the Euclidean ball of radius δ centered at $\boldsymbol{x}$, those domains have rounded corners. However, in practice, one can keep the stylized domains because the points outside the true interaction domains are not accessed during a finite element assembly process.

[3]The problem (4) is a nonlocal analogue of the PDE Poisson problem $-\nabla\cdot(\kappa\nabla u) = f_{\widehat{\Omega}}$ in $\widehat{\Omega}$, $u = g$ on a nonempty part of the boundary of $\widehat{\Omega}$, and $\kappa\nabla u\cdot\mathbf{n} = f_{Neumann}$ on the rest of that boundary.

the remainder of the paper. We refer to the domain Ω as being *semi-open* by which we mean that if $\partial\Omega$ and $\partial\Gamma$ denote the boundaries of Ω and Γ, respectively, Ω does not include the boundary portion $\partial\Omega \cap \partial\Gamma$ but does include the boundary portion $\partial\Omega \setminus (\partial\Omega \cap \partial\Gamma)$.

We define the function spaces

$$
\begin{cases}
W = \{v \in L^2(\Omega \cup \Gamma) \ : \ |||w||| < \infty\} \\
\qquad \text{where} \quad |||w|||^2 = \displaystyle\int_{\Omega\cup\Gamma}\int_{\Omega\cup\Gamma} |w(\boldsymbol{y}) - w(\boldsymbol{x})|^2 \gamma(\boldsymbol{x},\boldsymbol{y}) d\boldsymbol{y} d\boldsymbol{x} + \|w\|^2_{L^2(\Omega\cup\Gamma)} \\
W^0 = \{w \in W \ : \ w = 0 \text{ for } \boldsymbol{x} \in \Gamma\}
\end{cases} \tag{6}
$$

and, for $u, v \in W$, we define the bilinear form $\mathcal{A}(\cdot,\cdot)$ and linear functional $\mathcal{F}(\cdot)$ as

$$
\begin{cases}
\mathcal{A}(u,v) = \displaystyle\int_{\Omega\cup\Gamma}\int_{\Omega\cup\Gamma} \big(v(\boldsymbol{y}) - v(\boldsymbol{x})\big)\big(u(\boldsymbol{y}) - u(\boldsymbol{x})\big)\gamma(\boldsymbol{x},\boldsymbol{y}) d\boldsymbol{y} d\boldsymbol{x} \\
\mathcal{F}(v) = \displaystyle\int_{\Omega} v(\boldsymbol{x}) f(\boldsymbol{x}) d\boldsymbol{x}.
\end{cases} \tag{7}
$$

Then, a weak formulation of the nonlocal volume-constrained problem (5) can be stated as [18, 26, 27, 28]

$$
\begin{gathered}
\textit{given } f(\boldsymbol{x}) \in W', \ g(\boldsymbol{x}) \in W_\Gamma, \textit{ and a kernel } \gamma(\boldsymbol{x},\boldsymbol{y}), \textit{ find } u(\boldsymbol{x}) \in W \textit{ such that} \\
\mathcal{A}(u,v) = \mathcal{F}(v) \quad \forall\, v \in W^0 \qquad \textit{subject to } u(\boldsymbol{x}) = g(\boldsymbol{x}) \textit{ for } \boldsymbol{x} \in \Gamma.
\end{gathered} \tag{8}
$$

Here, W' denotes the dual space of bounded linear functionals on W^0 with respect to the standard L^2 duality pairing and W_Γ denotes the nonlocal "trace" space defined as $W_\Gamma = \{v|_\Gamma \ : \ v \in W\}$. If $\Gamma \neq \emptyset$, the well posedness of the problem (8) is proved in, e.g., [18, 26, 27, 28].

For $v \in W$, define the energy functional

$$
\mathcal{E}_{single}(v) = \frac{1}{2}\mathcal{A}(v,v) - \mathcal{F}(v). \tag{9}
$$

Then, (8) is equivalent to the minimization problem [18, 26, 27, 28]

$$
\begin{gathered}
\textit{given } f(\boldsymbol{x}) \in W', \ g(\boldsymbol{x}) \in W_\Gamma, \textit{ and a kernel } \gamma(\boldsymbol{x},\boldsymbol{y}), \textit{ find } u(\boldsymbol{x}) \in W \textit{ such that} \\
\mathcal{E}_{single}(u) = \inf_{v\in W} \mathcal{E}_{single}(v) \qquad \textit{subject to } u(\boldsymbol{x}) = g(\boldsymbol{x}) \textit{ for } \boldsymbol{x} \in \Gamma.
\end{gathered} \tag{10}
$$

Remark 1. The functional setting and the well posedness of the nonlocal problem depend on the kernel $\gamma(\boldsymbol{x},\boldsymbol{y})$. For example, if the kernel is square integrable (i.e., $\int_{\Omega\cup\Gamma} \big(\gamma(\boldsymbol{x},\boldsymbol{y})\big)^2 d\boldsymbol{y} < \infty$ for all $\boldsymbol{x} \in \Omega\cup\Gamma$) or if the kernel is integrable and translationally invariant (i.e., $\int_{\Omega\cup\Gamma} \gamma(\boldsymbol{x},\boldsymbol{y}) d\boldsymbol{y} < \infty$ for all $\boldsymbol{x} \in \Omega\cup\Gamma$ and $\gamma(\boldsymbol{x},\boldsymbol{y})) = \gamma(\boldsymbol{y}-\boldsymbol{x})$), it is known that $W = L^2(\Omega\cup\Gamma)$; see, e.g., [18, 26, 27, 28]. On the other hand, for the fractional kernel $\gamma(\boldsymbol{x},\boldsymbol{y}) \propto |\boldsymbol{y}-\boldsymbol{x}|^{-d-2s}$ with d denoting the space dimension and $0 < s < 1$, it is known that $W = H^s(\Omega\cup\Gamma)$, i.e., a fractional Sobolev space; again, see, e.g., [18, 26, 27, 28]. However, the technical aspects of this work are largely independent of the choice of the kernel as long as the nonlocal problem remains well-posed. Moreover, some conditions such as the symmetry of $\gamma(\boldsymbol{x},\boldsymbol{y})$ can be further relaxed under some additional assumptions [18, 19] that ensure the well-posedness of the nonlocal problem. Likewise, one can also relax the condition that $\gamma(\boldsymbol{x},\boldsymbol{y})$ be positive

everywhere; see, e.g., [39]. For such kernels, an energy minimization characterization of the problem may not be available, even though related strong and weak formulations are well defined. Thus, in particular, the algorithms developed in this work can be extended in a straightforward manner to problems that cannot be characterized in terms of an energy minimization setting. □

2.1. Finite element discretization of the nonlocal volume-constrained problem. The weak formulation (8) of the nonlocal volume-constrained problem can be discretized using a finite element method as follows. Let $\mathcal{T}^h$ denote a finite element triangulation of $\Omega \cup \Gamma$ parameterized by a grid-size parameter h. We assume that $\mathcal{T}^h$ conforms to the boundary of Ω, i.e., $\partial\Omega$ consists of finite element edges. This requirement can be satisfied by first constructing a grid in Ω after which a grid is constructed in Γ that shares element vertices with those of the grid in Ω along their common boundary. For simplicity, in the sequel, we restrict the discussion to Lagrangian finite element spaces.

Let $W^h \subset W$ and $W^{0,h} \subset W^0$ denote finite element (FE) subspaces. Then, a FE approximation $u^h(\boldsymbol{x}) \in W^h$ of the solution $u \in W$ of (8) is defined to be the solution of the discretized weak formulation

$$
\begin{aligned}
&\textit{given } f(\boldsymbol{x}) \in W',\ g(\boldsymbol{x}) \in W_\Gamma,\ \textit{and a kernel } \gamma(\boldsymbol{x},\boldsymbol{y}),\\
&\textit{find } u^h(\boldsymbol{x}) \in W^h \textit{ such that}\\
&\qquad \mathcal{A}(u^h, v^h) = \mathcal{F}(v^h) \quad \forall\, v^h \in W^{0,h} \qquad \textit{subject to } u^h(\boldsymbol{x}) = g^h(\boldsymbol{x}) \textit{ for } \boldsymbol{x} \in \Gamma,
\end{aligned} \tag{11}
$$

where $g^h(\boldsymbol{x})$ denotes an approximation of $g(\boldsymbol{x})$ that is usually chosen to be the FE interpolant[4] of $g(\boldsymbol{x})$. As long as $\Gamma \neq \emptyset$, the well posedness of problem (11) is also proved; see, e.g., [18, 26, 27, 28].

Let $\widetilde{N}^h$ denote the number of degrees of freedom corresponding to the nodes in $\Omega \cup \Gamma$ and let N_h denote the number of degrees of freedom corresponding to the (possibly semi-) open domain Ω, with the remaining and $\widetilde{N}^h - N^h$ degrees of freedom corresponding to the closed domain Γ. Note that because Ω is an open domain with respect to its common boundary with Γ and Γ itself is a closed domain, nodes and degrees of freedom along their common boundary are assigned to Γ. We then define the finite element subspace $W^h \subset W$ as the span of a nodal finite element basis $\{\phi_i(\boldsymbol{x})\}_{i=1}^{\widetilde{N}^h}$ so that a finite element approximation $u^h(\boldsymbol{x})$ of the solution $u(\boldsymbol{x})$ of (8) can be expressed as

$$
u^h(\boldsymbol{x}) = \sum_{i=1}^{N^h} (\vec{u})_i \phi_i(\boldsymbol{x}) + \sum_{i=N^h+1}^{\widetilde{N}^h} (\vec{g})_i \phi_i(\boldsymbol{x}), \tag{12}
$$

where $\vec{u}$ denotes an N^h-vector of unknown coefficients and $\vec{g}$ denotes an $(\widetilde{N}^h - N^h)$-vector of nodal values of the approximation $g^h(\boldsymbol{x})$ of $g(\boldsymbol{x})$. We recall that the support of each nodal basis function $\phi_i(\boldsymbol{x})$ comprises all elements sharing the node $\boldsymbol{x}_i$. As a result, all basis functions corresponding to nodes in Ω vanish on Γ and $\text{span}\{\phi_i(\boldsymbol{x})\}_{i=1}^{N^h} \subset W^{0,h}$.

Let $\mathbb{A}_{single}$ and $\vec{b}_{single}$ denote the $N^h \times N^h$ matrix and the N^h-vector with ele-

[4]When $g(\boldsymbol{x})$ is not of class C^0, $g^h(\boldsymbol{x})$ can be defined by, e.g., least-squares approximation or Clement interpolation [15].

ments

$$
\begin{cases} (\mathbb{A}_{single})_{ij} = \mathcal{A}(\phi_j, \phi_i) & \text{for } i,j = 1,\dots,N^h \\ (\vec{b}_{single})_i = \mathcal{F}(\phi_i) - \displaystyle\sum_{j=N^h+1}^{\widetilde{N}^h} \mathcal{A}(\phi_j,\phi_i)(\vec{g})_j & \text{for } i = 1,\dots,N^h, \end{cases} \tag{13}
$$

respectively. Then, the discrete FE problem (11) is equivalent to the linear algebraic system

$$
\mathbb{A}_{single}\vec{u} = \vec{b}_{single} \tag{14}
$$

for the unknown nodal coefficient vector $\vec{u}$. The matrix $\mathbb{A}_{single}$ is symmetric and, owing to the fact that $\Gamma \neq \emptyset$, it is also positive definite [1, 18, 26, 27, 28].

For $v^h \in W^h$, we define the discrete energy functional

$$
\mathcal{E}^h_{single}(v^h) = \frac{1}{2}\mathcal{A}(v^h, v^h) - \mathcal{F}(v^h). \tag{15}
$$

Then, the discrete nonlocal volume-constrained problem (11), respectively (14), can be expressed in terms of the equivalent minimization problem [18, 26, 27, 28]

$$
\begin{aligned} &\textit{the vector } \vec{u} \textit{ solves } (14) \iff u^h(\boldsymbol{x}) \in W^h \textit{ solves } (11) \iff \\ &\mathcal{E}^h_{single}(u^h(\boldsymbol{x})) = \min_{v^h(\boldsymbol{x})\in W^h} \mathcal{E}^h_{single}(v^h(\boldsymbol{x})) \quad \textit{subject to } v^h(\boldsymbol{x}) = g^h(\boldsymbol{x}) \text{ on } \Gamma. \end{aligned} \tag{16}
$$

REMARK 2. As implied by (3), any point $\boldsymbol{x} \in \Omega \cup \Gamma$ interacts only with points in the ball $B_\delta(\boldsymbol{x})$. This raises a serious issue in FE methods for nonlocal problems because the intersection of such balls and the finite element grid results in cut elements, i.e., partial elements, within the ball. As a result, one either has to deal with cut elements or, if one wants to only deal with uncut elements, one is faced with discontinuous integrands that vanish outside the ball. This issue is glossed over in many FE papers for nonlocal problems, especially those that only provide one-dimensional numerical results. However, we address this issue in Section 4.1. A comprehensive discussion of how to effectively handle cut elements can be found in [23]. □

3. Nonlocal domain decomposition in the continuous setting. In this section we first describe, in the continuous setting, how to define a nonlocal decomposition of the domain and then introduce the formulation of the multi-domain system. The central result of this section proves the equivalence of the solution of the single-domain system and the one corresponding to the multi-domain system. The significance of this result is that it establishes the consistency and the well posedness of our multi-domain formulation.

3.1. Construction of the geometric domain decomposition. In a standard PDE domain decomposition setting, one can partition Ω into non-overlapping subdomains and then simply define the subdomain problems by restricting the global operator to each subdomain. Such a construction is impossible in the nonlocal setting due to the inherent nonlocal interactions which require any two adjacent subdomains to share an interface having nonzero volume. As a result, our substructuring-based domain decomposition starts from a non-overlapping, covering subdivision of Ω into N_s subdomains $\{\widetilde{\Omega}_n\}_{n=1}^{N_s}$, as illustrated in Figure 2-left for $N_s = 6$, and then adds the overlaps necessary for the nonlocal interactions. Note that some of the domains

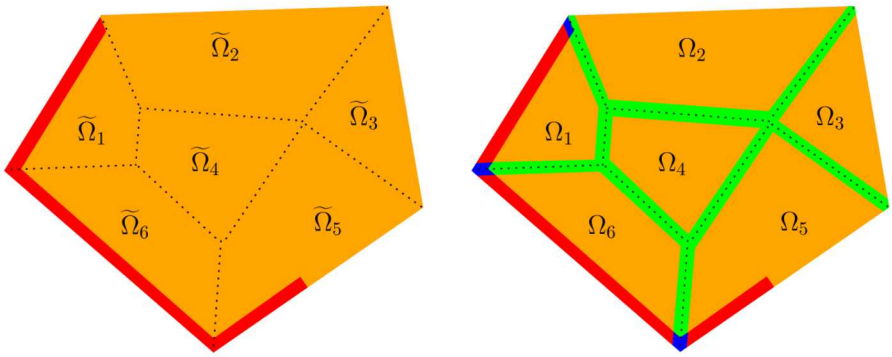

FIG. 2. *Left: a non-overlapping, covering subdivision of the domain Ω into six subdomains $\widetilde{\Omega}_n$, $n = 1, \ldots, N_s = 6$. Right: the corresponding nonlocal overlapping domain subdivision $\Omega_n \cup \widehat{\Gamma}_n$, $n = 1, \ldots, N_s = 6$. The domain $\cup_{n=1}^{6} \widehat{\Gamma}_n$ is depicted in green and the domain $\Gamma = \Gamma_1 \cup \Gamma_2 \cup \Gamma_5 \cup \Gamma_6$ is depicted in red with Γ_3 and Γ_4 being empty sets. The blue regions in Γ illustrate the overlaps between pairs of Γ_n.*

$\widetilde{\Omega}_n$ include part of the boundary $\partial\Omega$. For example, in Figure 2-left, we have that this is the case for $\widetilde{\Omega}_2$, $\widetilde{\Omega}_3$, and $\widetilde{\Omega}_5$ so that those are examples of what we refer to as semi-open subdomains because they are closed with respect to $\partial\Omega \setminus (\partial\Omega \cap \partial\Gamma)$.

For each subdomain $\widetilde{\Omega}_n$, $n = 1, \ldots, N_s$, we define the (possibly semi-) open smaller subdomain

$$\Omega_n = \left\{ \boldsymbol{x} \in \widetilde{\Omega}_n \;\; : \;\; |\boldsymbol{y} - \boldsymbol{x}| > \frac{\delta}{2} \quad \forall\, \boldsymbol{y} \in \Omega \setminus \widetilde{\Omega}_n \right\}; \tag{17}$$

see Figure 2-right for an illustration. Note that $\{\Omega_n\}_{n=1}^{N_s}$ is, by construction, a set of *non-overlapping* domains. We also subdivide the interaction domain Γ into a set of *overlapping*, covering subdomains

$$\Gamma_n = \left\{ \boldsymbol{x} \in \Gamma \;\; : \;\; |\boldsymbol{y} - \boldsymbol{x}| \leq \delta \quad \forall\, \boldsymbol{y} \in \Omega_n \right\} \qquad \text{for } n = 1, \ldots, N_s \tag{18}$$

and also define the set of *overlapping* subdomains

$$\widehat{\Gamma}_n = \left\{ \boldsymbol{x} \in \Omega \setminus \Omega_n \;\; : \;\; |\boldsymbol{y} - \boldsymbol{x}| \leq \delta \quad \forall \boldsymbol{y} \in \Omega_n \right\} \qquad \text{for } n = 1, \ldots, N_s. \tag{19}$$

In Figure 2-right, for each n, $\Gamma_n \cup \widehat{\Gamma}_n$ consists of all the strips of thickness δ that surround Ω_n, including in some instances a portion of Γ. Because each subdomain $\widehat{\Gamma}_n$ overlaps with at least one other subdomain $\widehat{\Gamma}_{n'}$, $n' \neq n$, and likewise for each subdomain Γ_n, the above construction results in the *overlapping* domain decomposition of $\Omega \cup \Gamma$ given by

$$\Omega \cup \Gamma = \cup_{n=1}^{N_s} \Omega_n \cup \widehat{\Gamma}_n \cup \Gamma_n. \tag{20}$$

Following conventional DD nomenclature, we subdivide the set of subdomains $\{\Omega_n \cup \widehat{\Gamma}_n \cup \Gamma\}_{n=1}^{N_s}$ into two classes:

$$\begin{aligned} \textit{floating subdomains} \quad & \text{if} \quad \Gamma_n = \emptyset \\ \textit{non-floating subdomains} \quad & \text{if} \quad \Gamma_n \neq \emptyset. \end{aligned}$$

For example, in Figure 2-right, Ω_3 and Ω_4 are floating subdomains, whereas Ω_1, Ω_2, Ω_5, and Ω_6 are non-floating. Analogous to the conventional local DD setting,

a floating domain is endowed with a purely Neumann nonlocal volume constraint so that its associated nonlocal problem has a non-trivial null space. In a typical local or nonlocal DD configuration, the number of subdomains is large and most of them are of the floating type.

REMARK 3. As alluded to in Section 1, in a local PDE setting one can consider both non-overlapping and overlapping DD algorithms because the latter offer some computational conveniences and may allow for a faster convergence of iterative solution methods. Typically, the overlap depends on the grid size and its thickness goes to zero as the mesh size is reduced. In contrast, the nonlocal setting *requires* any two adjacent subdomains to overlap in order to compute the necessary nonlocal interactions between them. As a result, the size of this *mandatory* overlap is determined not by the mesh size but by the interaction radius δ, i.e., its thickness is independent of the underlying discretization mesh. □

3.2. The domain decomposition (multi-domain) system. A multi-domain system is a system of N_s equations, each of which holds for $\boldsymbol{x} \in \Omega_n \cup \widehat{\Gamma}_n \cup \Gamma_n$, $n = 1, \ldots, N_s$. In constructing the multi-domain system we have to deal with overlapping domains, i.e., although the three domains $\cup_{n=1}^{N_s}\Omega_n$, $\cup_{n=1}^{N_s}\widehat{\Gamma}_n$, and $\cup_{n=1}^{N_s}\Gamma_n$ are mutually disjoint as are the N_s domains Ω_n, there are overlaps among the N_s domains in $\cup_{n=1}^{N_s}\Gamma_n$ and in $\cup_{n=1}^{N_s}\widehat{\Gamma}_n$.

To properly deal with the consequences of having overlapping domains, we define the functions

$$\zeta_{\mathcal{A}}(\boldsymbol{x},\boldsymbol{y}) = \sum_{n=1}^{N_s} \mathcal{X}_{\Omega_n\cup\widehat{\Gamma}_n\cup\Gamma_n}(\boldsymbol{x})\mathcal{X}_{\Omega_n\cup\widehat{\Gamma}_n\cup\Gamma_n}(\boldsymbol{y}) \quad \text{and} \quad \zeta_{\mathcal{F}}(\boldsymbol{x}) = \sum_{n=1}^{N_s} \mathcal{X}_{\Omega_n\cup\widehat{\Gamma}_n}(\boldsymbol{x}). \tag{21}$$

Note that $\zeta_{\mathcal{A}}(\boldsymbol{x},\boldsymbol{y})$ is a symmetric function, i.e., $\zeta_{\mathcal{A}}(\boldsymbol{x},\boldsymbol{y}) = \zeta_{\mathcal{A}}(\boldsymbol{y},\boldsymbol{x})$ and is a non-negative piecewise integer-valued function and $\zeta_{\mathcal{F}}(\boldsymbol{x})$ is a positive piecewise integer-valued function.

3.2.1. The subdomain system. For $n = 1, \ldots, N_s$ and any pair of functions $u_n(\boldsymbol{x})$ and $v_n(\boldsymbol{x})$ defined on $\Omega_n \cup \widehat{\Gamma}_n \cup \Gamma_n$, we define the subdomain bilinear form

$$\begin{aligned}&\mathcal{A}_n(u_n, v_n)\\ &= \int\limits_{\Omega_n\cup\widehat{\Gamma}_n\cup\Gamma_n} \int\limits_{\Omega_n\cup\widehat{\Gamma}_n\cup\Gamma_n} \zeta_{\mathcal{A}}(\boldsymbol{x},\boldsymbol{y})^{-1}\big(v_n(\boldsymbol{y}) - v_n(\boldsymbol{x})\big)\big(u_n(\boldsymbol{y}) - u_n(\boldsymbol{x})\big)\gamma(\boldsymbol{x},\boldsymbol{y})d\boldsymbol{y}d\boldsymbol{x}\end{aligned} \tag{22}$$

and the associated subdomain linear functional

$$\mathcal{F}_n(v_n) = \int_{\Omega_n\cup\widehat{\Gamma}_n} \zeta_{\mathcal{F}}(\boldsymbol{x})^{-1} v_n(\boldsymbol{x}) f(\boldsymbol{x}) d\boldsymbol{x}, \tag{23}$$

where, of course, for floating domains, i.e., if $\Gamma_n = \emptyset$, the integrals over Γ_n vanish.

For $n = 1, \ldots, N_s$, we define the function spaces

$$\begin{cases} W_n = \{w \in L^2(\Omega_n \cup \widehat{\Gamma}_n \cup \Gamma_n) \ : \ |||w|||_n < \infty\} \\ W_n^0 = \{w \in W_n \ : \ w = 0 \text{ for } \boldsymbol{x} \in \Gamma_n\}, \\ \qquad\qquad \text{where} \quad |||w|||_n^2 = \mathcal{A}_n(w,w) + \|w\|^2_{L^2(\Omega_n\cup\Gamma_n\cup\widehat{\Gamma}_n)}. \end{cases} \tag{24}$$

Let

$$\widetilde{W}_n = \begin{cases} W_n^0 & \text{if } \Gamma_n \neq \emptyset, \quad \text{i.e., for non-floating domains} \\ W_n & \text{if } \Gamma_n = \emptyset, \quad \text{i.e., for floating domains.} \end{cases} \tag{25}$$

We then define the *domain-decomposition* or *multi-domain* system of equations as

$$
\left\{
\begin{array}{l}
\textit{given } f(\boldsymbol{x}) \in W',\ g(\boldsymbol{x}) \in W_\Gamma,\ \textit{and a kernel } \gamma(\boldsymbol{x},\boldsymbol{y}),\\
\textit{for } n = 1,\dots,N_s,\ \textit{find } u_n \in W_n \ \textit{such that}\\
\quad \mathcal{A}_n(u_n, v_n) = \mathcal{F}_n(v_n) \quad \forall\, v_n \in \widetilde{W}_n \qquad (a)\\
\textit{subject to}\\
\quad u_n(\boldsymbol{x}) = u_{n'}(\boldsymbol{x}) \quad \forall\, \boldsymbol{x} \in \widehat{\Gamma}_n \cap \widehat{\Gamma}_{n'} \ \ \textit{for } n' = n+1,\dots,N_s \qquad (b)\\
\textit{and}\\
\quad u_n(\boldsymbol{x}) = g(\boldsymbol{x}) \quad \forall\, \boldsymbol{x} \in \Gamma_n \quad \textit{if } \Gamma_n \neq \emptyset,\ \textit{i.e., for non-floating domains.} \quad (c)
\end{array}
\right. \tag{26}
$$

Equation (26b) can be thought of as a nonlocal version of the standard continuity constraint in non-overlapping local DD methods. The constraints in that equation are needed because the solution $u(\boldsymbol{x})$ of (8) is a single-valued function on $\Omega \cup \Gamma$, and in particular on $\cup_{n=1}^{N_s} \widehat{\Gamma}_n$. However, by construction, we have that for all n' such that $\widehat{\Gamma}_n \cap \widehat{\Gamma}_{n'} \neq \emptyset$, both $u_n(\boldsymbol{x})$ and $u_{n'}(\boldsymbol{x})$ are defined on $\widehat{\Gamma}_n \cap \widehat{\Gamma}_{n'} \neq \emptyset$. Clearly, we have that (26b) must be imposed on that domain. Of course, this equation automatically holds on $\Gamma_n \cap \Gamma_{n'}$ because both $u_n(\boldsymbol{x}) = g(\boldsymbol{x})$ and $u_{n'}(\boldsymbol{x}) = g(\boldsymbol{x})$ there.

Remark 4. It is possible for $\zeta_{\mathcal{A}}(\boldsymbol{x},\boldsymbol{y}) = 0$. For example, this is the case if $\boldsymbol{x} \in \Omega_n$ and $\boldsymbol{y} \in \Omega_{n'}$ with $n' \neq n$. However, this fact does not cause problems in (22) because points $\boldsymbol{x}$ interact only with points $\boldsymbol{y}$ such that $|\boldsymbol{y}-\boldsymbol{x}| \leq \delta$ and for such pairs of points, $\zeta_{\mathcal{A}}(\boldsymbol{x},\boldsymbol{y}) > 0$. □

Remark 5. As in the standard (local) DD case, the constraints in (26b) ensure single-valued solutions of the multi-domain system, and are appropriate when the global nonlocal solution is also continuous. However, one of the principal advantages of nonlocal models is that, for some kernels in common use, they admit solutions with jump discontinuities [18, 26, 27, 28]. In anticipation of such solutions, one may choose to enforce (26b) weakly, i.e., i.e., for $n = 1,\dots,N_s$ and $n' = n+1,\dots,N_s$,

$$
\int_{\widehat{\Gamma}_n \cap \widehat{\Gamma}_{n'}} \big(u_n(\boldsymbol{x}) - u_{n'}(\boldsymbol{x})\big) v(\boldsymbol{x}) d\boldsymbol{x} = 0 \qquad \forall\, v(\boldsymbol{x}) \in W_n|_{\widehat{\Gamma}_n \cap \widehat{\Gamma}_{n'}}. \tag{27}
$$

Note that (27) also arises when (26b) is enforced using Lagrange multipliers; such a treatment of (26b) would therefore result in mass matrices being involved in finite element formulations of the constraints (26b). □

Remark 6. The constraints in (26b) are not independent. For example, consider a point $\boldsymbol{x} \in \widehat{\Gamma}_1 \cap \widehat{\Gamma}_4 \cap \widehat{\Gamma}_6$ near the bottom right corner of Ω_1 in Figure 2-right. Then, (26b) would include the constraints $u_1(\boldsymbol{x}) = u_4(\boldsymbol{x})$, $u_1(\boldsymbol{x}) = u_6(\boldsymbol{x})$, and $u_4(\boldsymbol{x}) = u_6(\boldsymbol{x})$, only two of which are independent. These redundancies in (26b) have implications in the design of discretization algorithms as is discussed in Section 4.2. □

3.2.2. Equivalence of the single-domain and multi-domain problems. Our next task is to show that the solution $u(\boldsymbol{x})$ for $\boldsymbol{x} \in \Omega \cup \Gamma$ of the single-domain system (8) and the solutions $u_n(\boldsymbol{x})$, $n = 1,\dots,N_s$, of the multi-domain system (26) are the same or, more precisely, that $u_n(\boldsymbol{x}) = u(\boldsymbol{x})$ for $\boldsymbol{x} \in \Omega_n \cup \widehat{\Gamma}_n \cup \Gamma_n$. The first step towards that end is the following lemma. We refer to Appendix A for a proof.

LEMMA 7. *Given functions $w(\boldsymbol{x})$ and $v(\boldsymbol{x})$ for $\boldsymbol{x} \in \Omega \cup \Gamma$, define the functions $w_n(\boldsymbol{x})$ and $v_n(\boldsymbol{x})$ for $\boldsymbol{x} \in \Omega_n \cup \widehat{\Gamma}_n \cup \Gamma_n$ as*

$$w_n(\boldsymbol{x}) = w(\boldsymbol{x})\big|_{\Omega_n \cup \widehat{\Gamma}_n \cup \Gamma_n} \quad \text{and} \quad v_n(\boldsymbol{x}) = v(\boldsymbol{x})\big|_{\Omega_n \cup \widehat{\Gamma}_n \cup \Gamma_n} \quad \text{for } n = 1, \ldots, N_s. \tag{28}$$

Then, for $n = 1, \ldots, N_s$ and $n' = n+1, \ldots, N_s$, we have that, if $\widehat{\Gamma}_n \cap \widehat{\Gamma}_{n'} \neq \emptyset$ and $\Gamma_n \cap \Gamma_{n'} \neq \emptyset$,

$$w_{n'}(\boldsymbol{x}) = w_n(\boldsymbol{x}) \;\; \text{and} \;\; v_{n'}(\boldsymbol{x}) = v_n(\boldsymbol{x}) \quad \text{for} \;\; \boldsymbol{x} \in \widehat{\Gamma}_n \cap \widehat{\Gamma}_{n'} \;\; \text{and} \;\; \boldsymbol{x} \in \Gamma_n \cap \Gamma_{n'}. \tag{29}$$

Then, for the bilinear forms and linear functionals defined in (7), (22), and (23), we have that

$$\mathcal{A}(w, v) = \sum_{i=1}^{N_s} \mathcal{A}_n(w_n, v_n) \qquad \text{and} \qquad \mathcal{F}(v) = \sum_{n=1}^{N_s} \mathcal{F}_n(v_n). \tag{30}$$

Using Lemma 7 and the fact that $W = \otimes_{n=1}^{N_s} W_n$ and $W^0 = \otimes_{n=1}^{N_s} \widetilde{W}_n$ one can easily prove the following equivalence result.

PROPOSITION 8. *Let $u(\boldsymbol{x}) \in W$ denote the solution of the single-domain system (8) and, for $n = 1, \ldots, N_s$, let $u_n(\boldsymbol{x}) \in W_n$ denote the solution of the n-th subproblem in multi-domain system (26). Then, the multi-domain system (26) and the single-domain system (8) are equivalent and their respective solutions coincide, i.e, $u_n(\boldsymbol{x}) = u(\boldsymbol{x})\big|_{\Omega_n \cup \widehat{\Gamma}_n \cup \Gamma_n}$.* □

The equivalence of the multi-domain and the global problems and the fact that the latter is well-posed implies that (26) is also well posed.

We note that the equivalence between the multi-domain weak formulation (26) and the single-domain system (8) can also be established by noting that the single-domain energy functional (9) can be written as a sum of subdomain energy functionals defining a multi-domain energy functional. The proof is straightforward so that it is omitted.

PROPOSITION 9. *Define the subdomain energy functionals $\mathcal{E}_n(u_n)$ by*

$$\mathcal{E}_n(u_n) := \frac{1}{2}\mathcal{A}_n(u_n, u_n) - \mathcal{F}_n(u_n) \qquad \text{for } n = 1, \ldots, N_s, \tag{31}$$

where the bilinear form $\mathcal{A}_n(\cdot, \cdot)$ and linear functional $\mathcal{F}_n(\cdot)$ are defined in (22) and (23), respectively. Then,

$$\sum_{n=1}^{N_s} \mathcal{E}_n(u_n) = \mathcal{E}_{single}(u). \tag{32}$$

Furthermore, the multi-domain weak formulation (26) is the Euler-Lagrange equation corresponding to the minimization problem

$$\inf_{v_n \in W_n,\, n=1,\ldots,N_s} \sum_{n=1}^{N_s} \mathcal{E}_n(v_n) \quad \begin{cases} \text{subject to, for } n, n' = 1, \ldots, N_s,\; n' \neq n, \\ u_n(\boldsymbol{x}) = u_{n'}(\boldsymbol{x}) \text{ for } \boldsymbol{x} \in \widehat{\Gamma}_n \cap \widehat{\Gamma}_{n'} \text{ and} \\ u_n(\boldsymbol{x}) = g(\boldsymbol{x}) \text{ for } \boldsymbol{x} \in \Gamma_n. \end{cases} \tag{33}$$

4. Finite element discretization of the subdomains systems. In this section we consider a finite element discretization corresponding to the multi-domain system (26). For finite element (FE) methods in general, the construction of the stiffness matrices and the right-hand side vectors corresponding to the subdomain problems follows a standard procedure which here we specialize to our setting. For each $n = 1, \ldots, N_s$, the procedure is given as follows.

Subdomain grid construction. From (22), it is clear that we need a meshing of the subdomain $\Omega_n \cup \Gamma_n \cup \widehat{\Gamma}_n$.

Definition of a finite element space. For each subdomain $\Omega_n \cup \Gamma_n \cup \widehat{\Gamma}_n$, we define a finite element space $\widetilde{W}_n^h$ as the span of a set of basis function, usually chosen to be piecewise polynomials with respect to whatever grid is constructed.

Definition of the sought for FE approximation. An approximation (of the solution $u_n(\boldsymbol{x})$ of (26)) having the form of a linear combination of the basis functions is then sought.

Discrete linear system construction. The stiffness matrix and right-hand side vector are constructed as is standard for nonlocal problems, i.e., in the same manner as that used for a single-domain problem.

It is crucial to keep in mind that this procedure, as is the case for DD methods in general, has as a central goal (2) that we rephrase more precisely as having

(34) *the global solution obtained from the* N_s discretized *subdomain FE systems corresponding to* (26)*, i.e.,* $u^{dd,h}(\boldsymbol{x})$*, should be the same as the solution* u^h *of the discretized single-domain FE system* (11)*.*

To meet this goal, it is obvious that the subdomain grids and subdomain basis functions have to be subsets of the grid and basis functions used for the single-domain problem. The implication is then that *the starting point for the construction of subdomain grids is a* given *single-domain grid.*[5]

4.1. Definition of subdomain grids. We assume we are given, as introduced in Section 2.1, a finite element meshing $\mathcal{T}^h$ of $\Omega \cup \Gamma$ that respects the common boundary shared by Ω and Γ. Associated with that mesh are $\widetilde{N}^h$ degrees of freedom, e.g., nodal values, N^h of which are associated with the domain Ω with the remaining $\widetilde{N}^h - N^h$ degrees of freedom associated with the closed domain Γ.

In *local* PDE settings, for both non-overlapping and overlapping DD methods, the next step is to subdivide the domain Ω into subdomains that contain only whole finite elements. If one is going to invoke a non-overlapping DD method, the construction of the subdomains is complete. If instead an overlapping DD method is to be used, one adds, to each non-overlapping subdomain, whole elements in neighboring subdomains that are within a certain distance from the common boundary between the two domains; the distance used is usually related to some multiple of the local grid size, although other criteria are also in use [12, 37, 51].

In the *nonlocal* case, the practical construction of a subdivision of Ω is similar to that for overlapping DD in the local case. We again start by subdividing Ω into the set $\{\widetilde{\Omega}_n\}_{n=1}^{N_s}$ of subdomains with each $\widetilde{\Omega}_n$ consisting of whole finite elements. We now want to add to and subtract from each subdomain $\widetilde{\Omega}_n$ strips of thickness $\delta/2$ to

[5]This approach precludes, in general, the use of the perhaps Utopian situation in which the domains $\{\Omega_n\}_{n=1}^{N_s}$, $\{\Gamma_n\}_{n=1}^{N_s}$, and $\{\widehat{\Gamma}_n\}_{n=1}^{N_s}$ are meshed separately into whole elements which respect their common boundaries. Utopia is reached in only the very simplest settings such as rectangular domains and Cartesian uniform meshes having a grid size proportional to δ.

create the subdomains Ω_n and $\widehat{\Gamma}_n$. Unfortunately, because we are given a global grid over $\Omega \cup \Gamma$ to work with, in general, we will not be able to (see Remark 2) define grids consisting of whole finite elements that respect the boundaries between Ω_n and $\widehat{\Gamma}_n$, i.e., those domains would also contain partial (cut) elements which is something we want to avoid.

We thus see that there is a big difference between the definitions of overlapping grids for the local and nonlocal cases. To recapitulate, in the local case we are free to add whole elements to effect an overlap with neighboring elements. In the nonlocal case, we do not have this freedom because the strips to be created have thickness δ irrespective of the given global finite element grid so that, in general, that strip will not consist of whole elements. Thus we have the choice of truncating triangles so that the δ thickness of the strip is respected or instead *approximate* the strip by a strip consisting of whole triangles which is tantamount to approximating the common boundaries of Ω_n and $\widehat{\Gamma}_n$ by element edges. We use the latter choice because it is substantially easier to implement and, as shown below, does not compromise achieving the goal (34).

The above discussion motivates the following procedure for the construction, in the discretized setting, of a subdivision of Ω into subdomains that is analogous, but not the same, as that in Section 3.1 for the continuous problem. We begin by assuming, as is done in Section 2.1 for the single-domain setting, that

– we are given an integer $N_s > 1$ and a finite element meshing $\mathcal{T}^h$ of $\Omega \cup \Gamma$ which respects their common boundary $\overline{\Omega} \cap \Gamma$.

We denote by $\mathcal{T}^h_\Omega$ and $\mathcal{T}^h_\Gamma$ the sets of finite elements in Ω and Γ, respectively, and we denote by T a typical element in $\mathcal{T}^h$. Then,

– we subdivide Ω into N_s non-overlapping, covering subdomains $\widetilde{\Omega}_n$, $n = 1, \ldots, N_s$, such that *each subdomain $\widetilde{\Omega}_n$ consists entirely of whole finite elements.*

This step is effected in entirely the same manner as for the local PDE non-overlapping DD setting so that no further comments are needed.

Note that the boundary $\partial\widetilde{\Omega}_n$ of $\widetilde{\Omega}_n$ consists of two or three disjoint, covering parts. First, we have for all n,

Type 1. $\sum_{n'=1,\, n' \neq n}^{N_s} \partial\widetilde{\Omega}_n \cap \partial\widetilde{\Omega}_{n'}$, i.e., the common boundary shared by $\widetilde{\Omega}_n$ and subdomains $\widetilde{\Omega}_{n'}$ that abut to $\widetilde{\Omega}_n$.

We also have either one or both of

Type 2. $\partial\widetilde{\Omega}_n \cap \partial\Gamma$, i.e., the common boundary shared by $\widetilde{\Omega}_n$ and Γ.

Type 3. $\partial\widetilde{\Omega}_n \setminus \left[\left(\sum_{n'=1,\, n' \neq n}^{N_s} \partial\widetilde{\Omega}_n \cap \partial\widetilde{\Omega}_{n'}\right)\right] \cup (\partial\widetilde{\Omega}_n \cap \partial\Gamma)$, i.e., the part of $\partial\widetilde{\Omega}_n$ that is not shared with the boundary of Γ or with any of the boundaries of other subdomains $\widetilde{\Omega}_{n'}$.

For example, referring to Figure 2-left, we have that the boundaries of floating domains such as $\widetilde{\Omega}_3$ consist of only Type 1 and 3 parts, the boundaries of domains such as $\widetilde{\Omega}_6$ consist of only Type 1 and 2 parts, and the boundaries of domains such as $\widetilde{\Omega}_5$ consists of all three parts.

Recall that, by construction, the domains $\widetilde{\Omega}_n$ consist of whole FE triangles. However, in general, the subdomains Ω_n, $\widehat{\Gamma}_n$, and Γ_n consist of whole FE triangles *and* additionally partial (cut) FE triangles. To obtain the equivalence of the single- and multi-domain FE solutions, we necessarily have to work with subdomains that consist of only whole FE triangles because only such triangles, i.e., triangles $T \in \mathcal{T}_h$, are used in the single-domain FE method. For this reason, we define an approach for the construction of subdomains Ω^h_n, $\widehat{\Gamma}^h_n$, and Γ^h_n of $\Omega \cup \Gamma$ in such a way that all subdomains consists of only whole FE triangles. Additionally, the construction process is required

account for all interactions that occur between two subdomains $\widetilde{\Omega}_n$ and $\widetilde{\Omega}_{n'}$. Meeting this requirement is guaranteed if all triangles that overlap with the $\widehat{\Gamma}_n$ are included in $\widehat{\Gamma}_n^h$.

The specific geometric domain decomposition we use is defined as follows. We denote by $\boldsymbol{x}^{vertex}$ a typical vertex on $\partial\widetilde{\Omega}_n$ and by $\boldsymbol{x}_T^{barycenter}$ the barycenter of a typical finite element $T \in \mathcal{T}^h$. Then, for $n = 1, \ldots, N_s$, we define the subdomains

$$
\begin{cases}
\widehat{\Gamma}_n^h = \big\{ T \in \mathcal{T}_\Omega^h \,:\, |\boldsymbol{x}^{vertex} - \boldsymbol{x}_T^{barycenter}| \le \dfrac{\delta}{2} + h \\
\qquad\qquad\qquad\qquad \forall\, \boldsymbol{x}^{vertex} \in \text{Type 1 part of } \partial\widetilde{\Omega}_n \big\} \\
\Omega_n^h = \big\{ T \in \widetilde{\Omega}_n \setminus (\widetilde{\Omega}_n \cap \widehat{\Gamma}_n^h) \big\} \\
\Gamma_n^h = \big\{ T \in \mathcal{T}_\Gamma^h \,:\, |\boldsymbol{x}^{vertex} - \boldsymbol{x}_T^{barycenter}| \le \delta + h \\
\qquad\qquad\qquad\qquad \forall\, \boldsymbol{x}^{vertex} \in \text{Type 2 part of } \partial\widetilde{\Omega}_n \big\}.
\end{cases}
\tag{35}
$$

We have that $\widehat{\Gamma}_n^h$ consists of all elements $T \in \mathcal{T}_\Omega^h$ whose barycenters are within a distance $\delta/2 + h$ of some element vertex on the Type 1 part of the boundary of $\widetilde{\Omega}_n$. Also, Γ_n^h consists of all elements $T \in \mathcal{T}_\Gamma^h$ whose barycenters are within a distance $\delta + h$ of some element vertex on the Type 2 part of the boundary of $\widetilde{\Omega}_n$. Note that this procedure guarantees that the true interface region $\widehat{\Gamma}_n$ is fully contained in the approximate interface region $\widehat{\Gamma}_n^h$. For obvious reasons, we refer to the approach we use as "barycenter-based".

We illustrate the above discussion in Figure 3. Note that all of that discussion applies even to the case of the single domain Ω being a rectangle and a single-domain FE grid that is Cartesian and uniform. Figure 3a depicts a portion of the grid in the single domain Ω that respects the common boundary (depicted by the thick line segment) between two subdomains $\widetilde{\Omega}_n$ and $\widetilde{\Omega}_{n'}$. For Figure 3b, we have that the orange subdomains depict portions of the subdomains Ω_n and $\Omega_{n'}$ and the blue domain depicts a portion of $\widehat{\Gamma}_n \cap \widehat{\Gamma}_{n'}$. Note that the common boundaries of both Ω_n and $\Omega_{n'}$ with $\widehat{\Gamma}_n \cap \widehat{\Gamma}_{n'}$ do not respect the grid so that Ω_n, $\Omega_{n'}$, and $\widehat{\Gamma}_n \cap \widehat{\Gamma}_{n'}$ all contain some partial (cut) triangles. Figure 3c illustrates the need to make changes to the single-domain FE grid so that the new grid does respect those common boundaries. Of course, if we define the subdomain FE discretization using the new grid of Figure 3c, there is no hope for the solution of the FE discretization of (26) to be the same as the solution of single-domain FE discretization (11), i.e., the goal (34) cannot be achieved. Note also that the re-meshing of Figure 3 is relatively easy to effect for Cartesian grids, but becomes a much more complex task for general grids, especially in three dimensions. Figure 3d illustrates the process defined in (35). Now the orange-shaded regions depict portions of the subdomains Ω_n^h and $\Omega_{n'}^h$ and the magenta region depicts a portion of $\widehat{\Gamma}_n^h \cap \widehat{\Gamma}_{n'}^h$. Note that, in Figure 3d, those three domains all contain only whole FE triangles. Also, the blue region in Figure 3b, i.e. $\widehat{\Gamma}_n \cap \widehat{\Gamma}_{n'}$, is fully contained in the set of magenta triangles.

Remark 10. Comparing the definitions of $\widehat{\Gamma}_n^h$, Γ_n^h, and Ω_n^h with the definitions of $\widehat{\Gamma}_n$, Γ_n, and Ω_n given in Section 3.1, one can certainly view the first trio as approximations to the second trio. However, this view does not intrude on any aspect of the developments that follow. For example, the accuracy of these domain approximations is, as is made evident in Section 4.2, irrelevant with respect to the goal stated in (34). □

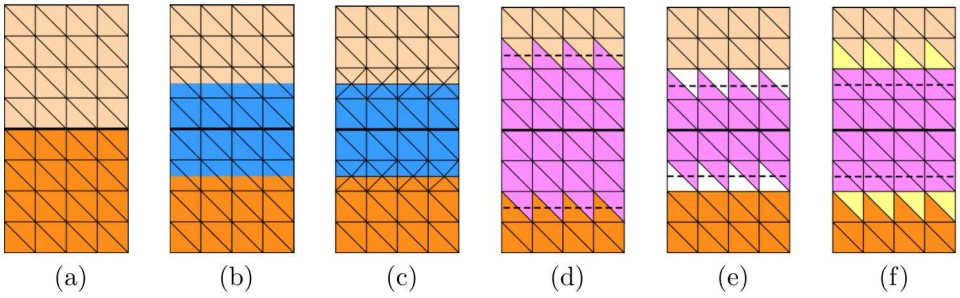

FIG. 3. *(a): A portion of the FE single-domain grid and portions of the two subdomains $\widetilde{\Omega}_n$ and $\widetilde{\Omega}_{n'}$. (b): Portions of the subdomains Ω_n and $\Omega_{n'}$ (in shades of orange) and of $\widehat{\Gamma}_n \cap \widehat{\Gamma}_{n'}$ (in blue). (c): A re-meshing of the FE grid of (a) so that now the common boundaries between the subdomains in (b) are respected but only if cut elements are introduced. (d): Portions of the approximate subdomains Ω_n^h and $\Omega_{n'}^h$ (in shades of orange) and of $\widehat{\Gamma}_n^h \cap \widehat{\Gamma}_{n'}^h$ (in magenta) as determined using (35). (e): The white elements overlap with $\widehat{\Gamma}_n$ but are not included in $\widehat{\Gamma}_n^h$. (f): The yellow elements are in $\widehat{\Gamma}_n^h \cap \widehat{\Gamma}_{n'}^h$ but do not overlap with $\widehat{\Gamma}_n \cap \widehat{\Gamma}_{n'}$.*

REMARK 11. Figure 3e illustrates why, e.g., in the first equation in (35), we used the criteria $|\boldsymbol{x}^{vertex} - \boldsymbol{x}_T^{barycenter}| \leq \frac{\delta}{2} + h$ and not simply the criteria $|\boldsymbol{x}^{vertex} - \boldsymbol{x}_T^{barycenter}| \leq \frac{\delta}{2}$. The barycenters of the white triangles are such that $|\boldsymbol{x}^{vertex} - \boldsymbol{x}_T^{barycenter}| > \frac{\delta}{2}$ so that using the latter criteria means that the white triangles are not included in $\widehat{\Gamma}_n^h$ even though it is obvious from Figure 3b that those triangles overlap with $\widehat{\Gamma}_n^h \cap \widehat{\Gamma}_{n'}^h$. On the other hand, Figure 3f illustrates that using the criteria $|\boldsymbol{x}^{vertex} - \boldsymbol{x}_T^{barycenter}| \leq \frac{\delta}{2} + h$ results in the yellow triangles which are in $\widehat{\Gamma}_n^h \cap \widehat{\Gamma}_{n'}^h$ but do not overlap with $\widehat{\Gamma}_n \cap \widehat{\Gamma}_{n'}$ so that those elements do not interact with elements on the other side of $\widehat{\Gamma}_n^h \cap \widehat{\Gamma}_{n'}^h$. However, the equivalence between single- and multi-domain solutions is not compromised because in assembling the FE stiffness matrix, the entries in that matrix corresponding to points in the yellow elements and points on the other side $\widehat{\Gamma}_n \cap \widehat{\Gamma}_{n'}$ are computed to be zero. □

4.2. Multi-domain finite element system. Let W^h denote the finite element space spanned by the set of basis functions $\{\phi_i(\boldsymbol{x})\}_{i=1}^{\widetilde{N}^h}$ used in Section (2.1) to define the single-domain FE system (14). Then, let

$$W_n^h = \text{span}\big\{ \cup_{i=1}^{\widetilde{N}^h} \phi_i(\boldsymbol{x}) \ : \ \boldsymbol{x}_i \in \Omega_n^h \cup \Gamma_n^h \cup \widehat{\Gamma}_n^h \big\} \qquad \text{for } n = 1, \ldots, N_s, \tag{36}$$

i.e., W_n^h is spanned by the basis functions ϕ_i such that the associated node $\boldsymbol{x}_i$ belongs to $\Omega_n^h \cup \Gamma_n^h \cup \widehat{\Gamma}_n^h$. The subspaces $W_n^h \subset W^h$ are well defined because of (35), i.e., because Ω_n^h, Γ_n^h, and $\widehat{\Gamma}_n^h$ all consist of whole elements from the triangulation $\mathcal{T}^h$. We also define the spaces

$$\begin{aligned} W_n^{0,h} = \big\{ w^h(\boldsymbol{x}) \in W_n^h \ : \ w^h(\boldsymbol{x}) = 0 \quad \text{for } \boldsymbol{x} \in \Gamma_n^h \big\} \\ \text{for } n = 1, \ldots, N_s \text{ such that } \Gamma_n^h \neq \emptyset. \end{aligned} \tag{37}$$

Note that *although we have that* $W_1^h \otimes \cdots \otimes W_{N_s}^h = W^h \subset W$, *in general,* $W_n^h \not\subset W_n$.

We define

$$\zeta_{\mathcal{A}}^h(\boldsymbol{x}, \boldsymbol{y}) = \sum_{n=1}^{N_s} \chi_{\Omega_n^h \cup \widehat{\Gamma}_n^h \cup \Gamma_n^h}(\boldsymbol{x}) \chi_{\Omega_n^h \cup \widehat{\Gamma}_n^h \cup \Gamma_n^h}(\boldsymbol{y}) \quad \text{and} \quad \zeta_{\mathcal{F}}^h(\boldsymbol{x}) = \sum_{n=1}^{N_s} \chi_{\Omega_n^h \cup \widehat{\Gamma}_n^h}(\boldsymbol{x}). \tag{38}$$

For $n = 1, \ldots, N_s$ and for $u_n^h(\boldsymbol{x})$, $v_n^h(\boldsymbol{x}) \in W_n^h$, we define the discretized subdomain bilinear form

$$\mathcal{A}_n^h(u_n^h, v_n^h) = \int\limits_{\Omega_n^h \cup \Gamma_n^h \cup \widehat{\Gamma}_n^h} \int\limits_{\Omega_n^h \cup \Gamma_n^h \cup \widehat{\Gamma}_n^h} \zeta_{\mathcal{A}}^h(\boldsymbol{x}, \boldsymbol{y})^{-1} \big(v_n^h(\boldsymbol{y}) - v_n^h(\boldsymbol{x})\big)\big(u_n^h(\boldsymbol{y}) - u_n^h(\boldsymbol{x})\big)\gamma(\boldsymbol{x}, \boldsymbol{y}) d\boldsymbol{y} d\boldsymbol{x} \tag{39}$$

and the discretized subdomain linear functional

$$\mathcal{F}_n^h(v_n^h) = \int_{\Omega_n^h \cup \widehat{\Gamma}_n^h} \zeta_{\mathcal{F}}^h(\boldsymbol{x})^{-1} v_n^h(\boldsymbol{x}) f(\boldsymbol{x}) d\boldsymbol{x} \tag{40}$$

with the tacit understanding that for floating domains, i.e., if $\Gamma_n^h = \emptyset$, the domains of integration of both integrals in (39) reduce to $\Omega_n^h \cup \widehat{\Gamma}_n^h$.

As done for the continuous problem, we introduce the function space

$$\widetilde{W}_n^h = \begin{cases} W_n^{0,h} & \text{if } \Gamma_n^h \neq \emptyset, \quad \textit{i.e., for non-floating domains} \\ W_n^h & \text{if } \Gamma_n^h = \emptyset, \quad \textit{i.e., for floating domains.} \end{cases}$$

Then, we define the system of equations

(41)

$$\begin{cases} \textit{given } f(\boldsymbol{x}) \in W', \ g(\boldsymbol{x}) \in W_\Gamma, \textit{ and a kernel } \gamma(\boldsymbol{x}, \boldsymbol{y}), \\ \textit{for } n = 1, \ldots, N_s, \textit{ find } u_n^h \in W_n^h \textit{ such that} \\ \quad \mathcal{A}_n^h(u_n^h, v_n^h) = \mathcal{F}_n^h(v_n^h) \qquad \forall\, v_n^h \in \widetilde{W}_n^h \qquad (a) \\ \textit{subject to} \\ \quad u_n^h(\boldsymbol{x}) = u_{n'}^h(\boldsymbol{x}) \quad \forall\, \boldsymbol{x} \in \widehat{\Gamma}_n^h \cap \widehat{\Gamma}_{n'}^h \ \textit{ for } n' = n+1, \ldots, N_s \qquad (b) \\ \textit{and} \\ \quad u_n^h(\boldsymbol{x}) = g^h(\boldsymbol{x}) \quad \forall\, \boldsymbol{x} \in \Gamma_n^h \quad \textit{if } \Gamma_n^h \neq \emptyset, \ \textit{i.e., for non-floating domains.} \quad (c) \end{cases}$$

The system (41) *is not a discretization of the system* (26) because $\mathcal{A}_n^h(\cdot,\cdot) \neq \mathcal{A}_n(\cdot,\cdot)$, i.e., the former is defined with respect to $\Omega_n^h \cup \Gamma_n^h \cup \widehat{\Gamma}_n^h$ whereas the latter is defined in terms of $\Omega_n \cup \Gamma_n \cup \widehat{\Gamma}_n$. However, this observation is unimportant because what is true is that

$$\begin{aligned} &\textit{the global discrete solution } u^{dd,h}(\boldsymbol{x}), \textit{ i.e. the solution such that} \\ &u_n^h(\boldsymbol{x}) = u^{dd,h}(\boldsymbol{x})|_{\Omega_n^h \cup \Gamma_n^h \cup \widehat{\Gamma}_n^h}, \textit{ is the same as the solution } u^h(\boldsymbol{x}) \\ &\textit{of the single-domain FE system } (11) \end{aligned} \tag{42}$$

which is, after all, the goal (34) we want to achieve. The truthfulness of (42) is verified following the same steps as those used to prove Proposition 8 with, of course, $\Omega_n \cup \Gamma_n \cup \widehat{\Gamma}_n$ replaced by $\Omega_n^h \cup \Gamma_n^h \cup \widehat{\Gamma}_n^h$.

When we define, in Section 4.2.1, the matrix form of (41), it is useful to differentiate between the bilinear forms in the two cases in (41a). First, because $\Gamma_n = \emptyset$ for *floating domains*, we have

$$\mathcal{A}_n^h(u_n^h, v_n^h) = \mathcal{A}_n^{fl,h}(u_n^h, v_n^h) = \int_{\Omega_n^h \cup \widehat{\Gamma}_n^h} \int_{\Omega_n^h \cup \widehat{\Gamma}_n^h} \zeta_{\mathcal{A}}^h(\boldsymbol{x}, \boldsymbol{y})^{-1} \big(v_n^h(\boldsymbol{y}) - v_n^h(\boldsymbol{x})\big)\big(u_n^h(\boldsymbol{y}) - u_n^h(\boldsymbol{x})\big)\gamma(\boldsymbol{x}, \boldsymbol{y}) d\boldsymbol{y} d\boldsymbol{x}. \tag{43}$$

For *non-floating domains*, the bilinear form involves integrals with respect to Γ_n^h. For such integrals, we have that either $v_n^h(\cdot) = 0$ [because $v_n^h \in W_n^{c,h}$] or $u_n^h(\cdot) = g^h(\cdot)$ [because of the constraint (41c)], so that then

$$\mathcal{A}_n^h(u_n^h, v_n^h) = \mathcal{A}_n^{nfl,h}(u_n^h, v_n^h) - \mathcal{A}_n^{g,h}(g^h, v_n^h), \tag{44}$$

where

$$\begin{aligned}
&\mathcal{A}_n^{nfl,h}(u_n^h, v_n^h) = \\
&\quad \int_{\Omega_n^h \cup \widehat{\Gamma}_n^h} \int_{\Omega_n^h \cup \widehat{\Gamma}_n^h} \zeta_{\mathcal{A}}^h(\boldsymbol{x}, \boldsymbol{y})^{-1} \big(v_n^h(\boldsymbol{y}) - v_n^h(\boldsymbol{x})\big)\big(u_n^h(\boldsymbol{y}) - u_n^h(\boldsymbol{x})\big)\gamma(\boldsymbol{x}, \boldsymbol{y}) d\boldsymbol{y} d\boldsymbol{x} \\
&\qquad + \int_{\Omega_n^h \cup \widehat{\Gamma}_n^h} \int_{\Gamma_n^h} \zeta_{\mathcal{A}}^h(\boldsymbol{x}, \boldsymbol{y})^{-1} u_n^h(\boldsymbol{x}) v_n^h(\boldsymbol{x}) d\boldsymbol{y} d\boldsymbol{x} \\
&\qquad + \int_{\Gamma_n^h} \int_{\Omega_n^h \cup \widehat{\Gamma}_n^h} \zeta_{\mathcal{A}}^h(\boldsymbol{x}, \boldsymbol{y})^{-1} u_n^h(\boldsymbol{y}) v_n^h(\boldsymbol{y}) d\boldsymbol{y} d\boldsymbol{x}
\end{aligned} \tag{45}$$

and

$$\begin{aligned}
\mathcal{A}_n^{g,h}(g^h, v_n^h) = &\int_{\Omega_n^h \cup \widehat{\Gamma}_n^h} \int_{\Gamma_n} \zeta_{\mathcal{A}}^h(\boldsymbol{x}, \boldsymbol{y})^{-1} g^h(\boldsymbol{y}) v_n(\boldsymbol{x}) d\boldsymbol{y} d\boldsymbol{x} \\
&+ \int_{\Gamma_n^h} \int_{\Omega_n^h \cup \widehat{\Gamma}_n^h} \zeta_{\mathcal{A}}({}^h\boldsymbol{x}, \boldsymbol{y})^{-1} g^h(\boldsymbol{x}) v_n^h(\boldsymbol{y}) d\boldsymbol{y} d\boldsymbol{x}.
\end{aligned} \tag{46}$$

Note that in (43), (45), and (46), both $u_n^h(\cdot)$ and $v_n^h(\cdot)$ are evaluated only at points in $\Omega_n^h \cup \widehat{\Gamma}_n^h$ and $g_n^h(\cdot)$ is evaluated only at points in Γ_n^h.

In light of (43), (45), and (46), (41) can be rewritten as, for *floating domains*,

$$\begin{cases} \mathcal{A}_n^{fl,h}(u_n^h, v_n^h) = \mathcal{F}_n^h(v_n^h) & (a) \\ u_n^h(\boldsymbol{x}) = u_{n'}^h(\boldsymbol{x}) \quad \forall\, \boldsymbol{x} \in \widehat{\Gamma}_n^h \cap \widehat{\Gamma}_{n'}^h \;\; \textit{for } n' = n+1, \ldots, N_s & (b) \end{cases} \tag{47}$$

and for *non-floating domains*

$$\begin{cases} \mathcal{A}_n^{nfl,h}(u_n^h, v_n^h) = \mathcal{F}_n^h(v_n^h) + \mathcal{A}_n^{g,h}(g^h, v_n^h) & (a) \\ u_n^h(\boldsymbol{x}) = u_{n'}^h(\boldsymbol{x}) \quad \forall\, \boldsymbol{x} \in \widehat{\Gamma}_n^h \cap \widehat{\Gamma}_{n'}^h \;\; \textit{for } n' = n+1, \ldots, N_s. & (b) \end{cases} \tag{48}$$

Remark 12. For any domain indexed by n, each of the subdomain problems in (47) and (48) is coupled, through (47)b or (48)b, to other domains indexed by n' with $n' \neq n$. Of course, this defeats the goal of domain decomposition which is to construct *uncoupled* subdomain problems so that, e.g., parallelization can be realized. This becomes the task for algorithms of obtaining *solutions* of the subdomain problems. Further comments in this regard are provided in Section 5. □

Remark 13. If instead of (4a) we consider

$$-2 \int_{\widehat{\Omega} \cup \Gamma \cup \Gamma_{Neumann}} \big(u(\boldsymbol{y}) - u(\boldsymbol{x})\big)\gamma(\boldsymbol{x}, \boldsymbol{y}) d\boldsymbol{y} + c(\boldsymbol{x}) u(\boldsymbol{x}) = f_{\widehat{\Omega}}(\boldsymbol{x})$$

with $c(\boldsymbol{x}) > 0$ so that the bilinear form $\mathcal{A}(u, v)$ in (7) has the additional term $\int_\Omega c(\boldsymbol{x}) u(\boldsymbol{x}) v(\boldsymbol{x}) d\boldsymbol{x}$, then that bilinear for is coercive even for floating subdomains. In this case, the design of solution methods for (41), and in particular for (47), becomes substantially simpler. □

Remark 14. The discussion that includes (43)–(48) as well as the comments made in Remarks 12 and 13 about the discrete bilinear form $\mathcal{A}_n^h(\cdot, \cdot)$ and the discrete subdomain system (41) also hold for the continuous bilinear form $\mathcal{A}_n(\cdot, \cdot)$ defined in (22) and continuous subdomain system (26). □

4.2.1. Matrix form of the multi-domain finite element system. Based on the numbering introduced in Section 2.1, we let

$X_{\Omega\cup\Gamma} = \{\boldsymbol{x}_i\}_{i=1}^{\widetilde{N}^h}$ denote the set of nodes in the grid used for the FE discretization of the single-domain $\Omega\cup\Gamma$

$X_\Omega = \{\boldsymbol{x}_i\}_{i=1}^{N^h}$ and $X_\Gamma = \{\boldsymbol{x}_i\}_{i=N^h+1}^{\widetilde{N}^h}$ denote the set of nodes in Ω and Γ, respectively.

The sets $X_\Omega \subset X_{\Omega\cup\Gamma}$ and $X_\Gamma \subset X_{\Omega\cup\Gamma}$ are disjoint and $X_\Omega \cup X_\Gamma = X_{\Omega\cup\Gamma}$. For $n = 1,\ldots,N_s$, let

$\widetilde{X}_n^h = \{\boldsymbol{x}_i^n\}_{i=1}^{\widetilde{N}_n^h}$ denote a local numbering of the set of nodes in $\Omega_n^h \cup \widehat{\Gamma}_n^h \cup \Gamma_n^h$; clearly, by construction, $\widetilde{X}_n^h \subset X_{\Omega\cup\Gamma}$

$X_n^h = \{\boldsymbol{x}_i^n\}_{i=1}^{N_n^h}$ and $X_{\Gamma_n^h}^h = \{\boldsymbol{x}_i^n\}_{N_n^h+1}^{\widetilde{N}_n^h}$ denote the nodes in $\widetilde{X}_n^h$ located in $\Omega_n^h \cup \widehat{\Gamma}_n^h$ and Γ_n^h, respectively.

The sets $X_n^h \subset \widetilde{X}_n^h$ and $X_{\Gamma_n^h}^h \subset \widetilde{X}_n^h$ are disjoint and $X_n^h \cup X_{\Gamma_n^h}^h = \widetilde{X}_n^h$. Note that for $n' \neq n$, the sets X_n^h and $X_{n'}^h$ overlap whenever $\widehat{\Gamma}_n^h \cap \widehat{\Gamma}_{n'}^h \neq \emptyset$ and similarly for the sets $X_{\Gamma_n^h}$ and $X_{\Gamma_{n'}^h}$. Also note that if Ω_n^h is a floating domain, then the set $X_{\Gamma_n}^h$ is vacuous.

Bilinear forms in matrix notation. We first consider the conversion of (47a) and (48a) to matrix notation. Corresponding to the nodes in $X_{\Omega\cup\Gamma}$, we have the set of basis functions $\{\phi_i(\boldsymbol{x})\}_{i=1}^{\widetilde{N}^h}$ whose span is used to define the finite element space W^h for the single-domain finite element system. We introduce the set of basis functions corresponding to each subdomain. For $n = 1,\ldots,N_s$, let

$\{\phi_i^n(\boldsymbol{x})\}_{i=1}^{\widetilde{N}_n^h}$ denote a local numbering of the basis functions in the spanning set for W^h which correspond to the nodes in $\widetilde{X}_n^h$.

By construction, $\{\phi_i^n(\boldsymbol{x})\}_{i=1}^{\widetilde{N}_n^h}$ spans the finite element space W_n^h. We then

divide $\{\phi_i^n(\boldsymbol{x})\}_{i=1}^{\widetilde{N}_n^h}$ into the sets $\{\phi_i^n(\boldsymbol{x})\}_{i=1}^{N_n^h}$ and $\{\phi_i^n(\boldsymbol{x})\}_{i=N_n^h+1}^{\widetilde{N}_n^h}$ that correspond to nodes in X_n^h and $X_{\Gamma_n^h}^h$, respectively.

Note that if Ω_n is a floating domain, then $N_n^h = \widetilde{N}_n^h$ so that the set $\{\phi_i^n(\boldsymbol{x})\}_{i=N_n^h+1}^{\widetilde{N}_n^h}$ is vacuous.

Let $\vec{u}_n$ denote an N_n^h-vector of nodal values of a function $u_n^h(\boldsymbol{x})$ defined for the nodes in X_n^h (i.e., nodes in $\Omega_n^h \cup \widehat{\Gamma}_n^h$) and let $\vec{g}_n$ denote the $(\widetilde{N}_n^h - N_n^h)$-vector of nodal values of $g^h(\boldsymbol{x})$ defined for the nodes in $X_{\Gamma_n^h}^h$ (i.e., nodes in Γ_n^h). Then, we have that

$$u_n^h(\boldsymbol{x}) = \begin{cases} \displaystyle\sum_{j=1}^{N_n^h} (\vec{u}_n)_j \phi_j^n(\boldsymbol{x}) + \sum_{j=N_n^h+1}^{\widetilde{N}_n^h} (\vec{g}_n)_j \phi_j^n(\boldsymbol{x}) & \textit{for non-floating domains} \\ \displaystyle\sum_{j=1}^{N_n^h} (\vec{u}_n)_j \phi_j^n(\boldsymbol{x}) & \textit{for floating domains.} \end{cases} \tag{49}$$

Note that components of $\vec{u}_n$ are ordered according the local indexing of nodes. We then define, for $n = 1,\ldots,N_s$, the entries of the $N_n^h \times N_n^h$ matrix $\mathbb{A}_n$ as

$$(\mathbb{A}_n)_{ij} = \begin{cases} \mathcal{A}_n^{nfl,h}(\phi_j^n, \phi_i^n) & \textit{for non-floating domains} \\ \mathcal{A}_n^{fl,h}(\phi_j^n, \phi_i^n) & \textit{for floating domains} \end{cases} \quad \text{for } i,j = 1,\ldots,N_n^h \tag{50}$$

and, for $i = 1, \dots, N_n^h$, the components of the N_n^h-vector $\vec{b}_n$ as

$$(\vec{b}_n)_i = \begin{cases} \mathcal{F}_n^h(\phi_i^n) - \displaystyle\sum_{j=N^h+1}^{\widetilde{N}^h} \mathcal{A}_n^{g,h}(\phi_j^n, \phi_i^n)(\vec{g}_n)_j & \textit{for non-floating domains} \\ \mathcal{F}_n^h(\phi_i^n) & \textit{for floating domains.} \end{cases} \tag{51}$$

Then, the finite element problems (47a) and (48a) both have the matrix-notation equivalent

$$\mathbb{A}_n \vec{u}_n = \vec{b}_n \qquad \text{for } n = 1, \dots, N_s. \tag{52}$$

Constraints in matrix notation. We next turn to the conversion of the constraints in (41b) [or equivalently (47b) and (48b)] to matrix notation.

We first transform those constraints to vector notation. We have global and local indices of nodes. Thus, if the node $\boldsymbol{x}_j^n \in X_n$ corresponds to the node $\boldsymbol{x}_i \in X$, i.e., if we have $\boldsymbol{x}_i = \boldsymbol{x}_j^n$, then i and j are the global and local indices, respectively, for the same node. We define a mapping from global to local indices, specifically, for a globally indexed node $\boldsymbol{x}_i \in \widehat{\Gamma}_n^h$, we let

$$I_{ni} = \textit{local index of the node } \boldsymbol{x}_i \in \widehat{\Gamma}_n^h.$$

Now suppose that $\widehat{\Gamma}_n^h \cap \widehat{\Gamma}_{n'}^h \neq \emptyset$. Then, for a globally indexed node $\boldsymbol{x}_i \in \widehat{\Gamma}_n^h \cap \widehat{\Gamma}_{n'}^h$, we have that

$$\boldsymbol{x}_i = \boldsymbol{x}_j^n = \boldsymbol{x}_{j'}^{n'} \qquad \text{where } j = I_{ni} \text{ and } j' = I_{n'i}.$$

Because the FE approximation $u_n^h(\boldsymbol{x})$ is uniquely determined by its nodal values, the constraints in (41b) can be equivalently expressed as

$$(\vec{u}_n)_j = (\vec{u}_{n'})_{j'} \quad \text{for all nodes} \quad \boldsymbol{x}_i \in \widehat{\Gamma}_n^h \cap \widehat{\Gamma}_{n'}^h, \quad n' = n+1, \dots, N_s. \tag{53}$$

We keep in mind that, as was the case for the continuous multi-domain system (see Remark 6), the constraints in (53) are not independent. For example, if $\widehat{\Gamma}_1^h \cap \widehat{\Gamma}_2^h \cap \widehat{\Gamma}_3^h \neq \emptyset$, then, for a node $\boldsymbol{x}_i$ in that domain, we have from (53) that $(\vec{u}_1)_j = (\vec{u}_2)_{j'}$, $(\vec{u}_1)_j = (\vec{u}_3)_{j''}$, and $(\vec{u}_2)_{j'} = (\vec{u}_3)_{j''}$, where $j = I_{1i}$, $j' = I_{2i}$, and $j'' = I_{3i}$. Cleary, these three equations are not independent.

Our task is then reduced to expressing the constraints in (53) in an economical matrix form. Here, we mimic the process given in [37] for DD in the local PDE case, In fact, we construct an $M \times \sum_{n=1}^{N_s} N_n^h$ matrix $\mathbb{M}$ of the form

$$\mathbb{M} = (\mathbb{M}_1 \cdots \mathbb{M}_{N_s})$$

such that the constraints in (53) can be equivalently expressed as

$$\sum_{n=1}^{N_s} \mathbb{M}_n \vec{u}_n = 0, \tag{54}$$

where $\mathbb{M}_n$, $n = 1, \dots, N_s$, are $M \times N_n^h$ matrices. We construct two such matrices, one for the constraints in (53), the other for an equivalent non-redundant set of constraints. To this end, letting $\widehat{\Gamma}^h = \cup_{n=1}^{N_s} \widehat{\Gamma}_n^h$,

$$\begin{aligned} &\textit{for each node in } \boldsymbol{x}_i \in \widehat{\Gamma}, \textit{ we define the set} \\ &\qquad \theta(\boldsymbol{x}_i) = \{n \ : \ \boldsymbol{x}_i \in \widehat{\Gamma}_n^h\} \\ &\textit{and let} \quad m(\boldsymbol{x}_i) = \textit{cardinality of the set } \theta(\boldsymbol{x}_i) \end{aligned} \tag{55}$$

so that $\theta(\boldsymbol{x}_i)$ consists of the indices of all the subdomains $\widehat{\Gamma}_n^h$ that contain the globally indexed node $\boldsymbol{x}_i$ and $m(\boldsymbol{x}_i)$ denotes the number of distinct subdomains which the node $\boldsymbol{x}_i$ belongs to.

Non-redundant constraints – full-rank matrix $\mathbb{M}$. For each node $\boldsymbol{x}_i \in \widehat{\Gamma}^h$,

- arrange the indices in $\theta(\boldsymbol{x}_i)$ in increasing order
- for each *consecutive* pair of indices, impose one constraint.

This results in, with $N_{\widehat{\Gamma}^h}$ denoting the number of nodes in $\widehat{\Gamma}^h$,

$$M = \sum_{i=1}^{N_{\widehat{\Gamma}^h}} \big(m(\boldsymbol{x}_i) - 1\big)$$

non-redundant constraints. For example, if $\widehat{\Gamma}_1^h \cap \widehat{\Gamma}_2^h \cap \widehat{\Gamma}_3^h \neq \emptyset$, then, for a node $\boldsymbol{x}_i$ in that domain, we now have that $(\vec{u}_1)_j = (\vec{u}_2)_{j'}$ and $(\vec{u}_2)_{j'} = (\vec{u}_3)_{j''}$, where $j = I_{1i}$, $j' = I_{2i}$, and $j'' = I_{3i}$. Clearly, these two equations are not redundant and together imply the constraint $(\vec{u}_1)_j = (\vec{u}_3)_{j''}$ from (53) that is now missing.

The entries of the matrix $\mathbb{M}$ can be determined as follows: set $k = 0$ and then,

- for $i = 1, \ldots, N_{\widehat{\Gamma}^h}$
- for each pair $n < n'$ of consecutive indices in $\theta(\boldsymbol{x}_i)$
- set $k \longleftarrow k + 1$
- set, for j and j' such that $\boldsymbol{x}_j^n = \boldsymbol{x}_{j'}^{n'} = \boldsymbol{x}_i$,

$$(\mathbb{M}_n)_{kj} = 1 \qquad (\mathbb{M}_{n'})_{kj'} = -1$$

and all other entries in the k-th row of $\mathbb{M}$ to zero.

Redundant constraints We proceed as we do above for the non-redundant set of constraints, except that now we do not require that $n < n'$ be consecutive indices in $\theta(\boldsymbol{x}_i)$, i.e., we impose a constraint for every distinct pair $n < n'$ of indices in $\theta(\boldsymbol{x}_i)$. This approach lends itself better for parallelization compared to the use of non-redundant constraints; see, e.g., [37] for a discussion in the local DD setting. Thus, we impose all the constraints in (53). Note that redundant constraints are caused only for $m_i(\boldsymbol{x}_i) \geq 3$. Because there are $m_i(\boldsymbol{x})$ distinct indices in $m(\boldsymbol{x}_i)$, we have that the number of rows in the matrix $\mathbb{M}$ is now given by

$$M = \sum_{i=1}^{N_{\widehat{\Gamma}^h}} \frac{1}{2} m(\boldsymbol{x}_i)\big(m(\boldsymbol{x}_i) - 1\big).$$

5. Concluding remarks. We have defined and analyzed a general framework for the construction of domain decomposition methods for nonlocal problems that achieves the goal stated in (2) or, more precisely, in (34). However, there is still work to be done because we have not met a second goal which is that the nonlocal DD method is amenable to parallelization. What we have so far are N_s systems (47)–(48) in which the subdomain systems are coupled through the constraints (47b) and (48b) or, equivalently, the subdomain matrix systems in (52) that are coupled through the constraints in (54). Such couplings prevent the direct use of (47)–(48) (or equivalently (52)–(54)) for achieving the second goal.

At a similar stage in the development DD algorithms in the local PDE setting, one is faced with the analogous situation; for example, in the non-overlapping DD setting, there is coupling of the subdomain problems at, say in the matrix formulation, at the nodes located along the common boundaries between subdomains. The uncoupling

between subdomain problems is then effected through the design of *solution methods* in which the bulk of the computational effort is borne by steps in those methods that are parallelizable and for which the non-paralellizable steps and the communications between subdomain problems, i.e., between processors, is kept to a minimum.

In the nonlocal DD setting, solution methods have to be designed to meet the same criterion: the bulk of the computational costs has to be borne by parallelizable steps. In a follow-up paper, we will develop, analyze, and implement such methods. Parallelizable solution methods for local PDE non-overlapping DD will be generalized to the nonlocal setting. For example, Lagrange multiplier methods, e.g., FETI [29], Arlequin methods [25], and optimization-based DD methods [32, 33, 34], all of which are in use for local PDE non-overlapping DD and which are also all good candidates for generalization to the nonlocal DD setting. Other local DD solution methods could also be considered for generalization. As is the case for the framework developed in this paper, generalizations of solution methods will pose challenges because of nonlocality. One thing to keep in mind is that a preferred solution method in the local setting may or may not remain so when generalized to the nonlocal setting.

Acknowledgments. Sandia National Laboratories is a multimission laboratory managed and operated by National Technology and Engineering Solutions of Sandia, LLC., a wholly owned subsidiary of Honeywell International, Inc., for the U.S. Department of Energy's National Nuclear Security Administration under contract DE-NA-0003525. This paper describes objective technical results and analysis. Any subjective views or opinions that might be expressed in the paper do not necessarily represent the views of the U.S. Department of Energy or the United States Government.

This work was supported by the Sandia National Laboratories (SNL) Laboratory-directed Research and Development (LDRD) program, and the U.S. Department of Energy, Office of Science, Office of Advanced Scientific Computing Research under Award Number DE-SC-0000230927 and under the Collaboratory on Mathematics and Physics-Informed Learning Machines for Multiscale and Multiphysics Problems (PhILMs) project.

REFERENCES

[1] B. Aksoylu and M. Parks, *Variational theory and domain decomposition for nonlocal problems*, Applied Mathematics and Computation, 217 (2011), pp. 6498–6515.

[2] B. Alali and M. Gunzburger, *Peridynamics and material interfaces*, Journal of Elasticity, 120 (2015), pp. 225–248.

[3] B. Alali and R. Lipton, *Multiscale dynamics of heterogeneous media in the peridynamic formulation*, Journal of Elasticity, 106 (2012), pp. 71–103.

[4] P. R. Amestoy, I. S. Duff, J.-Y. LExcellent, and J. Koster, *MUMPS: a general purpose distributed memory sparse solver*, in International Workshop on Applied Parallel Computing, Springer, 2000, pp. 121–130.

[5] H. Antil, E. Otarola, and A. Salgado, *Optimization with respect to order in a fractional diffusion model: Analysis, approximation and algorithmic aspects*, Journal of Scientific Computing, 77 (2018), pp. 204 – 224.

[6] H. Antil and M. Warma, *Optimal control of fractional semilinear PDEs*, ESAIM Control Optimisation and Calculus of Variations, (2019). To appear.

[7] E. Askari, *Peridynamics for multiscale materials modeling*, Journal of Physics: Conference Series, IOP Publishing, 125 (2008), pp. 649–654.

[8] S. Balay, S. Abhyankar, M. Adams, J. Brown, P. Brune, K. Buschelman, L. Dalcin, A. Dener, V. Eijkhout, W. Gropp, et al., *PETSc users manual*, (2019).

[9] D. Benson, S. Wheatcraft, and M. Meerschaert, *Application of a fractional advection-dispersion equation*, Water Resources Research, 36 (2000), pp. 1403–1412.

[10] A. Buades, B. Coll, and J. Morel, *Image denoising methods. A new nonlocal principle*, SIAM Review, 52 (2010), pp. 113–147.
[11] N. Burch, M. D'Elia, and R. Lehoucq, *The exit-time problem for a Markov jump process*, The European Physical Journal Special Topics, 223 (2014), pp. 3257–3271.
[12] X. Cai, *Overlapping domain decomposition methods*, in Advanced Topics in Computational Partial Differential Equations. Lecture Notes in Computational Science and Engineering, Springer, 33 (20003).
[13] G. Capodaglio, M. D'Elia, P. Bochev, and M. Gunzburger, *An energy-based coupling approach to nonlocal interface problems*, Computers and Fluids, (2019). To appear.
[14] Y. Chen, J. Lee, and A. Eskandarian, *Meshless methods in solid mechanics*, Springer Science & Business Media, 2006.
[15] P. Ciarlet, *The Finite Element Method for Elliptic Problems*, SIAM Classics in Applied Mathematics, SIAM, Philadelphia, 2002.
[16] C. Cortazar, M. Elgueta, J. Rossi, and N. Wolanski, *How to approximate the heat equation with Neumann boundary conditions by nonlocal diffusion problems*, Archive for Rational Mechanics and Analysis, 187 (2008), pp. 137–156.
[17] M. D'Elia, J.-C. De los Reyes, and A. Miniguano-Trujillo, *Bilevel parameter optimization for nonlocal image denoising models.* arXiv:1912.02347, 2019.
[18] M. D'Elia, Q. Du, C. Glusa, X. Tian, and Z. Zhou, *Numerical methods for nonlocal and fractional models*, ACTA Numerica, 29 (2020).
[19] M. D'Elia, Q. Du, M. Gunzburger, and R. Lehoucq, *Nonlocal convection-diffusion problems on bounded domains and finite-range jump processes*, Computational Methods in Applied Mathematics, 29 (2017), pp. 71–103.
[20] M. D'Elia, C. Glusa, and E. Otárola, *A priori error estimates for the optimal control of the integral fractional Laplacian*, SIAM Journal on Control and Optimization, 57 (2019), pp. 2775–2798.
[21] M. D'Elia and M. Gunzburger, *Optimal distributed control of nonlocal steady diffusion problems*, SIAM Journal on Control and Optimization, 55 (2014), pp. 667–696.
[22] M. D'Elia and M. Gunzburger, *Identification of the diffusion parameter in nonlocal steady diffusion problems*, Applied Mathematics and Optimization, 73 (2016), pp. 227–249.
[23] M. D'Elia, M. Gunzburger, and C. Vollman, *A cookbook for finite element methods for nonlocal problems, including quadrature rule choices and the use of approximate neighborhoods.* arXiv:2005.10775, 2020.
[24] M. D'Elia, X. Tian, and Y. Yu, *A physically-consistent, flexible and efficient strategy to convert local boundary conditions into nonlocal volume constraints*, SIAM Journal of Scientific Computing, 42 (2020), pp. A1935–A1949.
[25] H. Dhia and G. Rateau, *The Arlequin method as a flexible engineering design tool*, International Journal for Numerical Methods in Engineering, 62 (2005), pp. 1442–1462.
[26] Q. Du, *Nonlocal Modeling, Analysis, and Computation*, SIAM, 2019.
[27] Q. Du, M. Gunzburger, R. Lehoucq, and K. Zhou, *Analysis and approximation of nonlocal diffusion problems with volume constraints*, SIAM review, 54 (2012), pp. 667–696.
[28] Q. Du, M. Gunzburger, R. Lehoucq, and K. Zhou, *A nonlocal vector calculus, nonlocal volume-constrained problems, and nonlocal balance laws*, Mathematical Models and Methods in Applied Sciences, 23 (2013), pp. 493–540.
[29] C. Farhat and F.-X. Roux, *A method of finite element tearing and interconnecting and its parallel solution algorithm*, International Journal for Numerical Methods in Engineering, 32 (1991), pp. 1205–1227.
[30] G. Gilboa and S. Osher, *Nonlocal linear image regularization and supervised segmentation*, Multiscale Model. Simul., 6 (2007), pp. 595–630.
[31] M. Gulian, M. Raissi, P. Perdikaris, and G. E. Karniadakis, *Machine learning of space-fractional differential equations*, SIAM Journal on Scientific Computing, 41 (2019), pp. A2485–A2509.
[32] M. Gunzburger, M. Heinkenschloss, and H. Lee, *Solution of elliptic partial differential equations by an optimization-based domain decomposition method*, Applied Mathematics and Computation, 113 (2000), pp. 111 – 139.
[33] M. Gunzburger, J. Peterson, and H. Kwon, *An optimization based domain decomposition method for partial differential equations*, Computers & Mathematics with Applications, 37 (1999), pp. 77 – 93.
[34] P. Kuberry, P. Bochev, and K. Peterson, *An optimization-based approach for elliptic problems with interfaces*, SIAM Journal on Scientific Computing, 39 (2017), pp. S757–S781.
[35] T. Laursen and M. Heinstein, *Consistent mesh tying methods for topologically distinct dis-*

cretized surfaces in non-linear solid mechanics, International Journal for Numerical Methods in Engineering, 57 (2003), pp. 1197–1242.
[36] Y. Lou, X. Zhang, S. Osher, and A. Bertozzi, *Image recovery via nonlocal operators*, Journal of Scientific Computing, 42 (2010), pp. 185–197.
[37] T. Mathew, *Domain decomposition methods for the numerical solution of partial differential equations*, vol. 61, Springer Science & Business Media, 2008.
[38] M. Meerschaert and A. Sikorskii, *Stochastic models for fractional calculus*, Studies in mathematics, Gruyter, 2012.
[39] T. Mengesha and Q. Du, *Analysis of a scalar nonlocal peridynamic model with sign changing kernel*, Discrete Contin. Dyn. Syst. B, 18 (2013), pp. 1415–1437.
[40] R. Metzler and J. Klafter, *The random walk's guide to anomalous diffusion: a fractional dynamics approach*, Physics Reports, 339 (2000), pp. 1–77.
[41] R. Metzler and J. Klafter, *The restaurant at the end of the random walk: recent developments in the description of anomalous transport by fractional dynamics*, Journal Physics A, 37 (2004), pp. 161–208.
[42] G. Pang, M. D'Elia, M. Parks, and G. E. Karniadakis, *nPINNs: nonlocal Physics-Informed Neural Networks for a parametrized nonlocal universal Laplacian operator. Algorithms and Applications*, Journal of Computational Physics, (2020). To appear.
[43] G. Pang, L. Lu, and G. E. Karniadakis, *fPINNs: Fractional physics-informed neural networks*, SIAM Journal on Scientific Computing, 41 (2019), pp. A2603–A2626.
[44] G. Pang, P. Perdikaris, W. Cai, and G. E. Karniadakis, *Discovering variable fractional orders of advection–dispersion equations from field data using multi-fidelity Bayesian optimization*, Journal of Computational Physics, 348 (2017), pp. 694 – 714.
[45] M. Parks, L. Romero, and P. Bochev, *A novel lagrange-multiplier based method for consistent mesh tying*, Computer Methods in Applied Mechanics and Engineering, 196 (2007), pp. 3335 – 3347.
[46] L. Sabatelli, S. Keating, J. Dudley, and P. Richmond, *Waiting time distributions in financial markets*, European Physics Journal B, 27 (2002), pp. 273–275.
[47] E. Scalas, R. Gorenflo, and F. Mainardi, *Fractional calculus and continuous time finance*, Physica A, 284 (2000), pp. 376–384.
[48] A. Schekochihin, S. Cowley, and T. Yousef, *MHD turbulence: Nonlocal, anisotropic, nonuniversal?*, in IUTAM Symposium on computational physics and new perspectives in turbulence, Springer, Dordrecht, 2008, pp. 347–354.
[49] R. Schumer, D. Benson, M. Meerschaert, and B. Baeumer, *Multiscaling fractional advection-dispersion equations and their solutions*, Water Resources Research, 39 (2003), pp. 1022–1032.
[50] R. Schumer, D. Benson, M. Meerschaert, and S. Wheatcraft, *Eulerian derivation of the fractional advection-dispersion equation*, Journal of Contaminant Hydrology, 48 (2001), pp. 69–88.
[51] A. Toselli and O. Widlund, *Domain decomposition methods-algorithms and theory*, vol. 34, Springer Science & Business Media, 2006.
[52] H. You, Y. Yu, N. Trask, M. Gulian, and M. D'Elia, *Data-driven learning of robust nonlocal physics from high-fidelity synthetic data.* arXiv:2005.10076, 2020.

Appendix A. Proof of Lemma 7.

It is convenient for what follows to introduce, for each $n = 1, \dots, N_s$ such that $\Gamma_n \neq \emptyset$, the splitting

$$\Gamma_n = \Gamma_n^* \cup \Gamma_n^\dagger \quad \text{with} \quad \begin{cases} \Gamma_n^* \subset \Gamma_n \quad \text{such that} \quad \Gamma_n^* \cap (\cup_{n'=1,\, n' \neq n}^{N_s} \Gamma_{n'}) = \emptyset \\ \Gamma_n^\dagger = \Gamma_n \setminus \Gamma_n^* \subset \Gamma_n \end{cases}$$

so that Γ_n^* (resp. $\Gamma_n^\dagger$) are the disjoint parts of Γ_n that do not (resp. do) overlap with any other $\Gamma_{n'}$ with $n' \neq n$. The blue regions in Figure 2-right illustrate examples of the sets $\Gamma_n^\dagger$. Note that, by definition, $\Gamma_n^* \cap \Gamma_n^\dagger = \emptyset$. With these definitions in hand, we have that, for $n = 1, \dots, N_s$, $\Omega_n \cup \widehat{\Gamma}_n \cup \Gamma_n = \Omega_n \cup \widehat{\Gamma}_n \cup \Gamma_n^* \cup \Gamma_n^\dagger$. We can then express (21) as

$$\zeta_{\mathcal{A}}(\boldsymbol{x}, \boldsymbol{y}) = \sum_{n=1}^{N_s} \mathcal{X}_{\Omega_n \cup \Gamma_n^* \cup \widehat{\Gamma}_n \cup \Gamma_n^\dagger}(\boldsymbol{x}) \mathcal{X}_{\Omega_n \cup \Gamma_n^* \cup \widehat{\Gamma}_n \cup \Gamma_n^\dagger}(\boldsymbol{y}).$$

Note that among the sets Ω_n, Γ_n^*, $\widehat{\Gamma}_n$, and $\Gamma_n^\dagger$ the only two that may possibly overlap with other sets are $\Gamma_n^\dagger$ and $\widehat{\Gamma}_n$. For this reason and for ease of notation, we further introduce the set $\widetilde{\Gamma}_n = \Gamma_n^\dagger \cup \widehat{\Gamma}_n$. Based on this consideration, we split the outer integral of the bilinear form $\mathcal{A}_n$ into a set that does not overlap with any other sets (i.e. $\Omega_n \cup \Gamma_n^*$) and $\widetilde{\Gamma}_n$. We have:

$$\begin{aligned}
&\mathcal{A}_n(u_n, v_n) \\
&\quad = \int_{\Omega_n \cup \Gamma_n^* \cup \widetilde{\Gamma}_n} \int_{\Omega_n \cup \Gamma_n^* \cup \widetilde{\Gamma}_n} \zeta_{\mathcal{A}}(\mathbf{x}, \mathbf{y})^{-1} \big(v_n(\mathbf{y}) - v_n(\mathbf{x})\big)\big(u_n(\mathbf{y}) - u_n(\mathbf{x})\big)\gamma(\mathbf{x}, \mathbf{y}) d\mathbf{y} d\mathbf{x} \\
&\quad = \mathcal{A}_n^{disjoint}(u_n, v_n) + \mathcal{A}_n^{overlap}(u_n, v_n),
\end{aligned}$$

where

$$\begin{aligned}
&\mathcal{A}_n^{disjoint}(u_n, v_n) := \\
&\qquad \int_{\Omega_n \cup \Gamma_n^*} \int_{\Omega_n \cup \Gamma_n^* \cup \widetilde{\Gamma}_n} \zeta_{\mathcal{A}}(\mathbf{x}, \mathbf{y})^{-1} \big(v_n(\mathbf{y}) - v_n(\mathbf{x})\big)\big(u_n(\mathbf{y}) - u_n(\mathbf{x})\big)\gamma(\mathbf{x}, \mathbf{y}) d\mathbf{y} d\mathbf{x}, \\
&\mathcal{A}_n^{overlap}(u_n, v_n) := \\
&\qquad \int_{\widetilde{\Gamma}_n} \int_{\Omega_n \cup \Gamma_n^* \cup \widetilde{\Gamma}_n} \zeta_{\mathcal{A}}(\mathbf{x}, \mathbf{y})^{-1} \big(v_n(\mathbf{y}) - v_n(\mathbf{x})\big)\big(u_n(\mathbf{y}) - u_n(\mathbf{x})\big)\gamma(\mathbf{x}, \mathbf{y}) d\mathbf{y} d\mathbf{x}.
\end{aligned}$$

To simplify the notation, we let $w_n(\boldsymbol{x}, \boldsymbol{y}) = \big(u_n(\mathbf{y}) - u_n(\mathbf{x})\big)\gamma(\mathbf{x}, \mathbf{y})$ and $\big(u(\mathbf{y}) - u(\mathbf{x})\big)\gamma(\mathbf{x}, \mathbf{y}) = w(\boldsymbol{x}, \boldsymbol{y})$. Note that whenever $\boldsymbol{x}$ or $\boldsymbol{y}$ belong to a set that overlaps with other sets, the interface conditions guarantee that $w_n(\boldsymbol{x}, \boldsymbol{y}) = w(\boldsymbol{x}, \boldsymbol{y})$. We first analyze $\mathcal{A}_n^{disjoint}$; we have that

$$\begin{aligned}
\mathcal{A}_n^{disjoint}(u_n, v_n) &= \int_{\Omega_n \cup \Gamma_n^*} \int_{\Omega_n \cup \Gamma_n^* \cup \widetilde{\Gamma}_n} w(\mathbf{x}, \mathbf{y}) d\boldsymbol{y} d\boldsymbol{x} \\
&= \int_{\Omega_n \cup \Gamma_n^*} \int_{\Omega_n \cup \Gamma_n^* \cup \widetilde{\Gamma}_n} w(\mathbf{x}, \mathbf{y}) d\boldsymbol{y} d\boldsymbol{x} \\
&\quad + \int_{\Omega_n \cup \Gamma_n^*} \int_{(\Omega \cup \Gamma) \setminus (\Omega_n \cup \Gamma_n^* \cup \widetilde{\Gamma}_n)} w(\mathbf{x}, \mathbf{y}) d\mathbf{y} d\mathbf{x}
\end{aligned}$$

where the first equality follows from the fact that $\zeta_{\mathcal{A}}(\mathbf{x}, \mathbf{y}) = 1$ for $\mathbf{x} \in \Omega_n \cup \Gamma_n^*$ and $\boldsymbol{y} \in \Omega_n \cup \Gamma_n^* \cup \widetilde{\Gamma}_n$ and the second inequality from the fact that $\gamma(\mathbf{x}, \mathbf{y}) = 0$ for $\mathbf{x} \in \Omega_n \cup \Gamma_n^*$ and $\boldsymbol{y} \in (\Omega \cup \Gamma) \setminus (\Omega_n \cup \Gamma_n^* \cup \widetilde{\Gamma}_n)$. Hence,

$$\sum_{n=1}^{N_s} \mathcal{A}_n^{disjoint}(u_n, v_n) = \int_{\bigcup_{n=1}^{N_s} (\Omega_n \cup \Gamma_n^*)} \int_{\Omega \cup \Gamma} w(\mathbf{x}, \mathbf{y}) d\mathbf{y} d\mathbf{x}. \tag{56}$$

By definition of $\zeta_{\mathcal{A}}$, for any $\mathbf{y} \in (\Omega_n \cup \Gamma_n^*)$ and for any $\mathbf{x} \in \widetilde{\Gamma}_n$ we have $\zeta_{\mathcal{A}}(\mathbf{x}, \mathbf{y}) = 1$, hence

$$\begin{aligned}
\mathcal{A}_n^{overlap}(u_n, v_n) &= \int_{\widetilde{\Gamma}_n} \int_{\Omega_n \cup \Gamma_n^*} \big(v_n(\mathbf{y}) - v_n(\mathbf{x})\big)\big(u_n(\mathbf{y}) - u_n(\mathbf{x})\big)\gamma(\mathbf{x}, \mathbf{y}) d\mathbf{y} d\mathbf{x} \\
&\quad + \int_{\widetilde{\Gamma}_n} \int_{\widetilde{\Gamma}_n} \zeta_{\mathcal{A}}(\mathbf{x}, \mathbf{y})^{-1} \big(v_n(\mathbf{y}) - v_n(\mathbf{x})\big)\big(u_n(\mathbf{y}) - u_n(\mathbf{x})\big)\gamma(\mathbf{x}, \mathbf{y}) d\mathbf{y} d\mathbf{x} \\
&= \mathcal{A}_n^{overlap,I}(u_n, v_n) + \mathcal{A}_n^{overlap,II}(u_n, v_n).
\end{aligned}$$

We introduce an open disjoint covering $\{\Lambda_i\}_{i=1}^{N_\lambda}$ of $\bigcup_{n=1}^{N_s}\widetilde{\Gamma}_n$, i.e.

$$\bigcup_{i=1}^{N_\lambda}\Lambda_i=\bigcup_{i=1}^{N_s}\widetilde{\Gamma}_n,\quad\text{and}\quad\Lambda_i\cap\Lambda_j=\emptyset,\ \text{for } i\neq j,$$

such that there exists an index set I_n, $n=1,\dots N_s$, for which

$$\bigcup_{i\in I_n}\Lambda_i=\widetilde{\Gamma}_n.$$

In practice, this means that for every $n=1,\dots N_s$ there exists a subset of the covering that provides a disjoint covering of $\widetilde{\Gamma}_n$. Note that such a disjoint covering always exists. Then we have

$$\begin{aligned}\sum_{n=1}^{N_s}\mathcal{A}_n^{overlap,I}(u_n,v_n)&=\sum_{n=1}^{N_s}\int_{\widetilde{\Gamma}_n}\int_{\Omega_n\cup\Gamma_n^*}w_n(\mathbf{x},\mathbf{y})d\mathbf{y}d\mathbf{x}\\&=\sum_{n=1}^{N_s}\sum_{i\in I_n}\int_{\Lambda_i}\int_{\Omega_n\cup\Gamma_n^*}w_n(\mathbf{x},\mathbf{y})d\mathbf{y}d\mathbf{x}\\&=\sum_{n=1}^{N_s}\sum_{i=1}^{N_\lambda}\int_{\Lambda_i}\int_{\Omega_n\cup\Gamma_n^*}w_n(\mathbf{x},\mathbf{y})d\mathbf{y}d\boldsymbol{x}\\&=\sum_{i=1}^{N_\lambda}\int_{\Lambda_i}\left[\sum_{n=1}^{N_s}\int_{\Omega_n\cup\Gamma_n^*}w_n(\mathbf{x},\mathbf{y})d\boldsymbol{y}\right]d\boldsymbol{x}\\&=\int_{\bigcup_{n=1}^{N_s}\widetilde{\Gamma}_n}\int_{\bigcup_{n=1}^{N_s}(\Omega_n\cup\Gamma_n^*)}w(\mathbf{x},\mathbf{y})d\mathbf{y}d\mathbf{x},\end{aligned}$$

where the second equality follows from the fact that $\{\Lambda_i\}_{i\in I_n}$ form a disjoint covering of $\widetilde{\Gamma}_n$, the third from the fact that $\gamma(\boldsymbol{x},\boldsymbol{y})=0$ for all the extra terms, the fourth from the fact that the sums are independent and hence can be switched, and the fifth from the fact that the sets are disjoint.

For $\mathcal{A}_n^{overlap,II}$ we have

$$\begin{aligned}\sum_{n=1}^{N_s}\mathcal{A}_n^{overlap,II}(u_n,v_n)&=\sum_{n=1}^{N_s}\int_{\widetilde{\Gamma}_n}\int_{\widetilde{\Gamma}_n}\zeta_A(\boldsymbol{x},\boldsymbol{y})^{-1}w(\boldsymbol{x},\boldsymbol{y})d\mathbf{y}d\mathbf{x}\\&=\sum_{n=1}^{N_s}\sum_{i\in I_n}\sum_{j\in I_n}\int_{\Lambda_i}\int_{\Lambda_j}\zeta_A(\boldsymbol{x},\boldsymbol{y})^{-1}w(\boldsymbol{x},\boldsymbol{y})d\mathbf{y}d\mathbf{x},\end{aligned}$$

where, again, the second inequality follows from the fact that the sets $\{\Lambda_i\}_{i\in I_n}$ are disjoint and form a covering of $\widetilde{\Gamma}_n$.

Next, we introduce the index set $\mathcal{I}_{ij}(\boldsymbol{x},\boldsymbol{y})$ that contains all indexes n such that $(\boldsymbol{x},\boldsymbol{y})\in\Lambda_i\times\Lambda_j$ and $i,j\in I_n$. Formally,

$$\mathcal{I}_{ij}(\boldsymbol{x},\boldsymbol{y})=\{n\in\{1,\dots,N_s\}\text{ s.t. }\boldsymbol{x}\in\Lambda_i,\ \boldsymbol{y}\in\Lambda_j,\text{ and } i,\ j\in I_n\}.\tag{57}$$

We let cardinality$(\mathcal{I}_{ij})(\boldsymbol{x},\boldsymbol{y})=\mu_{ij}(\boldsymbol{x},\boldsymbol{y})$; this is the number of times the pair $(\boldsymbol{x},\boldsymbol{y})\in\Lambda_i\times\Lambda_j$ is considered when solving all subproblems, i.e.

$$\mu_{ij}(\boldsymbol{x},\boldsymbol{y})=\sum_{n=1}^{N_s}\mathcal{X}(n\in\mathcal{I}_{ij}(\boldsymbol{x},\boldsymbol{y})).$$

Note that for $\boldsymbol{x} \in \Lambda_i$ and $\boldsymbol{y} \in \Lambda_j$

$$\begin{aligned}\zeta_{\mathcal{A}}(\boldsymbol{x},\boldsymbol{y}) &= \sum_{n=1}^{N_s} \mathcal{X}_{\Omega_n \cup \Gamma_n^* \cup \widetilde{\Gamma}_n}(\boldsymbol{x}) \mathcal{X}_{\Omega_n \cup \Gamma_n^* \cup \widetilde{\Gamma}_n}(\boldsymbol{y}) \\ &= \sum_{n=1}^{N_s} \mathcal{X}(n \in \mathcal{I}_{ij}(\boldsymbol{x},\boldsymbol{y})) \mathcal{X}_{\Lambda_i}(\boldsymbol{x}) \mathcal{X}_{\Lambda_j}(\boldsymbol{y}) \\ &= \sum_{n=1}^{N_s} \mathcal{X}(n \in \mathcal{I}_{ij}(\boldsymbol{x},\boldsymbol{y})) = \mu_{ij}(\boldsymbol{x},\boldsymbol{y}).\end{aligned} \tag{58}$$

Thus,

$$\begin{aligned}\sum_{n=1}^{N_s} \mathcal{A}_n^{overlap,II}(u_n, v_n) &= \sum_{n=1}^{N_s} \sum_{i \in I_n} \sum_{j \in I_n} \int_{\Lambda_i} \int_{\Lambda_j} \zeta_A(\boldsymbol{x},\boldsymbol{y})^{-1} w(\boldsymbol{x},\boldsymbol{y}) d\boldsymbol{y} d\boldsymbol{x} \\ &= \sum_{n=1}^{N_s} \sum_{i \in I_n} \sum_{j \in I_n} \int_{\Lambda_i} \int_{\Lambda_j} \mathcal{X}(n \in \mathcal{I}_{ij}(\boldsymbol{x},\boldsymbol{y})) \mathcal{X}_{\Lambda_i}(\boldsymbol{x}) \mathcal{X}_{\Lambda_j}(\boldsymbol{y}) \zeta_A(\boldsymbol{x},\boldsymbol{y})^{-1} w(\boldsymbol{x},\boldsymbol{y}) d\boldsymbol{y} d\boldsymbol{x} \\ &= \sum_{n=1}^{N_s} \sum_{i=1}^{N_\lambda} \sum_{j=1}^{N_\lambda} \int_{\Lambda_i} \int_{\Lambda_j} \mathcal{X}(n \in \mathcal{I}_{ij}(\boldsymbol{x},\boldsymbol{y})) \mathcal{X}_{\Lambda_i}(\boldsymbol{x}) \mathcal{X}_{\Lambda_j}(\boldsymbol{y}) \zeta_A(\boldsymbol{x},\boldsymbol{y})^{-1} w(\boldsymbol{x},\boldsymbol{y}) d\boldsymbol{y} d\boldsymbol{x} \\ &= \sum_{i=1}^{N_\lambda} \sum_{j=1}^{N_\lambda} \int_{\Lambda_i} \int_{\Lambda_j} \zeta_A(\boldsymbol{x},\boldsymbol{y}) \zeta_A(\boldsymbol{x},\boldsymbol{y})^{-1} w(\boldsymbol{x},\boldsymbol{y}) d\boldsymbol{y} d\boldsymbol{x} \\ &= \int_{\bigcup_{n=1}^{N^s} \widetilde{\Gamma}_n} \int_{\bigcup_{n=1}^{N^s} \widetilde{\Gamma}_n} w(\boldsymbol{x},\boldsymbol{y}) d\boldsymbol{y} d\boldsymbol{x}.\end{aligned}$$

Here, in the second equality we only added terms that are equal to 1 because all the indicator functions are active. This allows us to extend the sums over i and j in the third equality because all the extra terms are zero. Then, the fourth equality follows from (58) and the fifth from the fact that all sets Λ_i and Λ_j are disjoint.

It then follows that

$$\begin{aligned}\sum_{n=1}^{N_s} \mathcal{A}_n^{overlap}(u_n, v_n) &= \sum_{n=1}^{N_s} \Big(\mathcal{A}_n^{overlap,I}(u_n, v_n) + \mathcal{A}_n^{overlap,II}(u_n, v_n) \Big) \\ &= \int_{\bigcup_{n=1}^{N_s} \widetilde{\Gamma}_n} \Big(\int_{\bigcup_{n=1}^{N_s} (\Omega_n \cup \Gamma_n^*)} w(\mathbf{x},\mathbf{y}) d\mathbf{y} + \int_{\bigcup_{n=1}^{N_s} \widetilde{\Gamma}_n} w(\mathbf{x},\mathbf{y}) d\mathbf{y} \Big) d\mathbf{x} \\ &= \int_{\bigcup_{n=1}^{N_s} \widetilde{\Gamma}_n} \int_{\Omega \cup \Gamma} w(\mathbf{x},\mathbf{y}) d\mathbf{y} d\mathbf{x}.\end{aligned} \tag{59}$$

The last equality follows from the fact that $\bigcup_{n=1}^{N_s} (\Omega_n \cup \Gamma_n^*)$ and $\bigcup_{n=1}^{N_s} (\Gamma_n^\dagger \cup \widehat{\Gamma}_n)$ are two disjoint sets. For the same reason, we have

$$\begin{aligned}\sum_{n=1}^{N_s} \mathcal{A}_n(u_n, v_n) &= \sum_{n=1}^{N_s} \Big(\mathcal{A}_n^{disjoint}(u_n, v_n) + \mathcal{A}_n^{overlap}(u_n, v_n) \Big) \\ &\int_{\bigcup\limits_{n=1}^{N_s} (\Omega_n \cup \Gamma_n^*)} \int_{\Omega \cup \Gamma} w(\mathbf{x},\mathbf{y}) d\mathbf{y} d\mathbf{x} + \int_{\bigcup_{n=1}^{N_s} \widetilde{\Gamma}_n} \int_{\Omega \cup \Gamma} w(\mathbf{x},\mathbf{y}) d\mathbf{y} d\mathbf{x} \\ &= \int_{\Omega \cup \Gamma} \int_{\Omega \cup \Gamma} w(\mathbf{x},\mathbf{y}) d\mathbf{y} d\mathbf{x} = \mathcal{A}(u, v).\end{aligned} \tag{60}$$

The proof for $\mathcal{F}$ directly follows from the same arguments and it is not reported.

Appendix B. Numerical tests for a FETI formulation. Numerical simulations have been conducted to validate the theoretical analysis presented in the paper and illustrate the consistency and robustness of the proposed nonlocal domain-decomposition strategy. Specifically, we illustrate Proposition 8 that states that the solution of the single-domain problem and the one obtained from the solution of the multi-domain problem are equivalent.

We point out that in these preliminary tests we consider the special case of simple rectangular domains discretized by structured grids; furthermore, we choose δ such that $\delta = ch$ for some positive integer $c \geq 1$. This is a restrictive choice, although standard in several meshfree settings.

Solution strategy We solve the multi-domain system with a FETI-like approach (see [29] for the local counterpart), as outlined in Remark 5 in the paper, i.e. we prescribe the coupling conditions weakly as follows:

$$\int_{\widehat{\Gamma}_n \cap \widehat{\Gamma}_{n'}} \big(u_n(\boldsymbol{x}) - u_{n'}(\boldsymbol{x})\big)\mu(\boldsymbol{x})d\boldsymbol{x} = 0 \qquad \forall\, \mu \in W_n|_{\widehat{\Gamma}_n \cap \widehat{\Gamma}_{n'}}. \tag{61}$$

Note that in FETI approaches the test function μ in (61) plays the role of a Lagrange multiplier and is part of the unknowns.

Discretization We discretize the multi-domain problem via finite element method using piecewise linear finite element spaces for both the solution of the single-domain problem, the solutions of the multi-domain problem and the Lagrange multipliers.

Software The matrix assembly is performed using the C++ finite element library FEMuS [6], built on top of the PETSc library [8]. The solution of the multi-domain system is obtained either with the same library, or with Matlab. In the former case, the system is solved in a monolithic fashion using the MUMPS direct solver [4]. In the latter case, we first solve for the Lagrange multipliers and then for the sub-solutions with a Schur complement approach.

Notation and problem set up In all our tests we denote by u^h the approximate finite element solution of the single-domain problem and by $u^{h,dd}$ the one obtained from the solution of the multi-domain problem. According to the strategies described in the previous paragraph, we denote by $u_F^{h,dd}$ and $u_M^{h,dd}$ the solutions computed with FEMuS and Matlab respectively. We also introduce the vectors $\vec{y}_F$ and $\vec{y}_M$ that correspond to the nodal values of the solutions and multipliers corresponding to $u_F^{h,dd}$ and $u_M^{h,dd}$ respectively. We consider the following subdomain configurations:

- **C1** Four subdomains with Dirichlet volume constraints, see Figure 4.
- **C2** Two subdomains for a cantilever beam domain, i.e. one domain with mixed (Dirichlet-Neumann) volume constraints and one domain with Neumann constraints only, see Figure 5.
- **C3** Two subdomains with a floating subdomain fully contained in the other domain to which Dirichlet volume constraints are prescribed, see Figure 6.

Results for C1 Note the absence of floating subdomains, i.e. the multi-domain problem does not require any special treatment since its matrix is non-singular. Let the (single) domain be defined as $\Omega = [-1, 1]\times[-0.5, 0.5]$ and let $\Omega\cup\Gamma = [-1.25, 1.25]\times$

[6] `http://github.com/gcapodag/MyFEMuS`

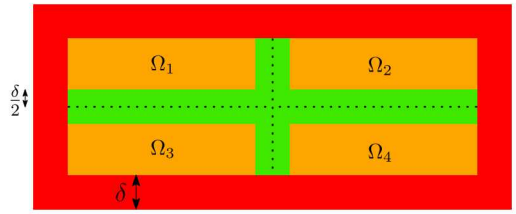

FIG. 4. *Four-subdomain configuration without floating subdomains,* **C1**.

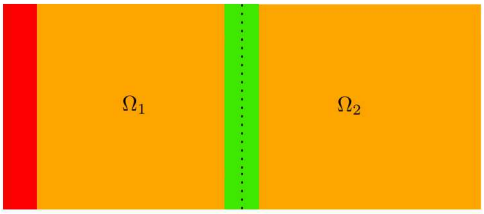

FIG. 5. *Two-subdomain configuration with a floating domain,* **C2**.

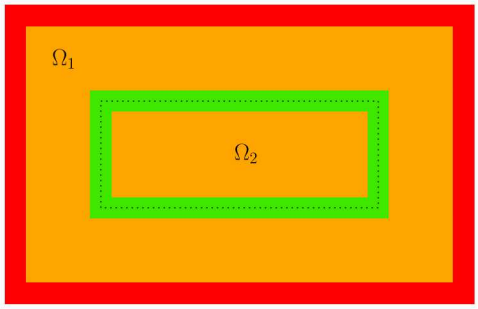

FIG. 6. *Two-subdomain configuration with a floating domain Ω_2 fully contained in Ω_1,* **C3**.

$[-0.75, 0.75]$, i.e. $\delta = 0.25$. The mesh size is set to $h = 0.0625$. In Figure 7 we show the computational domain Ω in blue, the computational interaction domain Γ in red and the finite element quadrilateral grid. These are decomposed in four subdomains as shown in Figure 4. The finite element solutions for the single-domain and multi-domain problem are compared in Figure 8.

Numerical errors are reported in Table 1, first row. Here, we report, respectively in each column, the L^2 norm of $(u^h - u_F^{h,dd})$, the ℓ^2 norm of the difference of their nodal values, i.e. $(\vec{u} - \vec{u}_F)$, and the ℓ^2 norm of $(\vec{y}_F - \vec{y}_M)$. Results show that all these errors are zero up to machine precision; hence, the single-domain and multi-domain solutions are equivalent, regardless of the solver used for their computation, confirming the theoretical results.

Results for C2 Note that in this configuration the right subdomain is floating (physical and virtual interaction domains are of Neumann type), hence, the multi-domain matrix is singular and special care must be taken when solving the system. The (single) computational domain, computational interaction domain and quadrilateral grid are the same as in **C1**, see Figure 7. In Figure 9, left, we report the single-domain finite element solution u; on the right, we report a line plot at $y = 0$ of the sub-solutions, denoted by u_1 and u_2. Note that u_1 and u_2 are set to zero outside

	$\|u^h - u_F^{h,dd}\|_{L^2}$	$\|\vec{u} - \vec{u}_F\|_{\ell^2}$	$\|\vec{y}_F - \vec{y}_M\|_{\ell^2}$
C1	1.10e−15	2.00e−14	2.78e−14
C2	5.85e−14	9.60e−13	1.70e−11
C3	1.80e−15	2.00e−14	2.30e−12

TABLE 1
Errors between solutions.

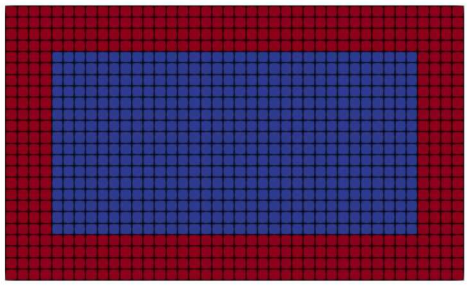

FIG. 7. *Domain, interaction domain and quadrilateral grid for the configurations* **C1** *and* **C2**.

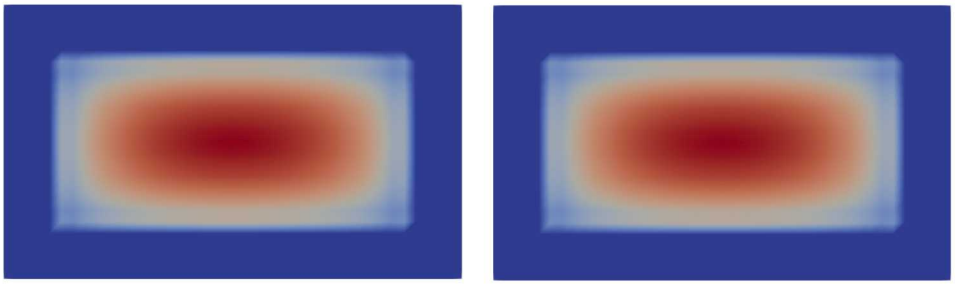

FIG. 8. *For configuration* **C1**, *finite element solutions* $u^{h,dd}$ *(left) and* u^h *(right).*

their respective subdomains. The numerical errors are reported in Table 1, middle

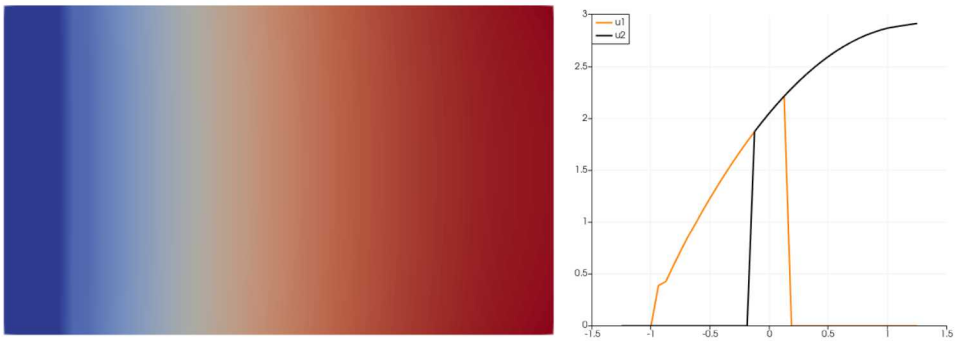

FIG. 9. *For configuration* **C2**, u^h *on the left; line plot at* $y = 0$ *of* u_1 *and* u_2 *on the right.*

row. Once again, the errors are zero up to machine precision. This confirms the suitability of the proposed formulation also in presence of floating subdomains.

Results for C3 In this test we consider a different domain for the single-domain problem, we let $\Omega = [-2.2.] \times [-1.5, 1.5]$ and $\Omega \cup \Gamma = [-2.25, 2.25] \times [-1.75, 1.75]$, i.e. $\delta = 0.25$. The mesh size is set to $h = 0.125$. In this test a floating subdomain is fully contained in Ω, as illustrated in Figure 6. In Figure 10 we report the single-domain solution u^h on the left and the sub-solutions u_1 and u_2 in the middle and on the right respectively. The numerical results reported in Table 1, bottom row, show the same error behavior as for cases **C1** and **C2**. We conclude that the proposed approach is consistent also in the realistic case of floating subdomains fully contained in the single-domain.

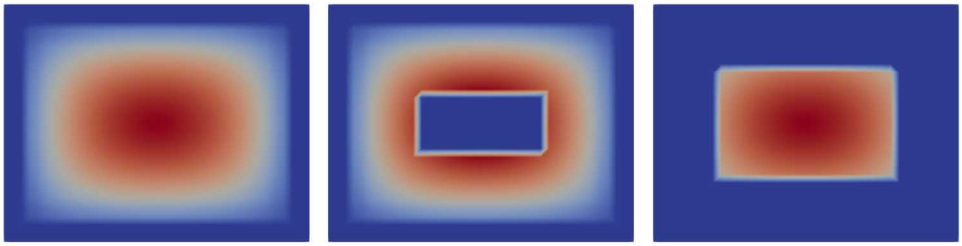

FIG. 10. *Solutions for* **C3**. *Left: global solution. Middle:* u_1. *Right* u_2.